



Cite this: *RSC Med. Chem.*, 2020, 11, 184

Received 9th October 2019,  
Accepted 26th November 2019

DOI: 10.1039/c9md00479c

rsc.li/medchem

## An epigrammatic status of the ‘azole’-based antimalarial drugs

Mousmee Sharma<sup>bc</sup> and Parteek Prasher<sup>id</sup>\*<sup>ac</sup>

The development of multidrug resistance in the malarial parasite has sabotaged majority of the eradication efforts by restraining the inhibition profile of first line as well as second line antimalarial drugs, thus necessitating the development of novel pharmaceuticals constructed on appropriate scaffolds with superior potency against the drug-resistant and drug-susceptible *Plasmodium* parasite. Over the past decades, the infectious malarial parasite has developed resistance against most of the contemporary therapeutics, thus necessitating the rational development of novel approaches principally focused on MDR malaria. This review presents an epigrammatic collation of the epidemiology and the contemporary antimalarial therapeutics based on the ‘azole’ motif.

### 1. Introduction

Vector-borne diseases are infections transmitted by mosquitoes, flies, and ticks that transfer contagious pathogens such as virus, bacteria, and protozoa from one host to the other.<sup>1</sup> In the early 1940s, the discovery of synthetic insecticides and the adoption of large-scale indoor spraying programs<sup>2</sup> led to the eradication of most vector-borne diseases. However, due to inconsistent control programs and dearth of vector control experts and qualified entomologists, the diseases soon re-emerged<sup>3</sup> in the form of resistant strains against contemporary insecticides.<sup>4</sup> As

per the latest reports by the World Health Organization (WHO), vector-borne diseases account for around 17% of all the infectious diseases that claim close to a million deaths annually.<sup>5</sup> Apparently, diseases like malaria account for 2 billion registered cases that claim around 0.4 million deaths annually.<sup>6</sup> The current antimalarial therapy relying upon artemisinin, antifolates, and quinine-based chemotherapy has been proven to be futile primarily against two of the four human malaria parasite species, viz., *P. falciparum*<sup>7</sup> and *P. vivax*,<sup>8</sup> whereas the multidrug-resistance (MDR) phenomenon is not well established in *P. malariae* or *P. ovale*.<sup>9</sup> Besides, multiple other factors, apart from drug resistance, also contribute to the failure of antimalarial therapy and these include misdiagnosis, non-compliance with the duration of dosing regimen, poor drug interactions that lead to erratic absorption, and irregular dosing.<sup>10</sup> As a result, antimalarial chemotherapy has witnessed

<sup>a</sup> Department of Chemistry, University of Petroleum & Energy Studies, Dehradun 248007, India. E-mail: pprasher@ddn.upes.ac.in, parteekchemistry@gmail.com

<sup>b</sup> Department of Chemistry, Uttarakhand University, Dehradun 248007, India

<sup>c</sup> UGC Sponsored Centre for Advanced Studies, Department of Chemistry, Guru Nanak Dev University, Amritsar 143005, India



Mousmee Sharma

and playing badminton.

Dr. Mousmee Sharma is currently employed as Assistant Professor in the Department of Chemistry, Uttarakhand University, Dehradun. She did her doctorate from Guru Nanak Dev University, India in the year 2019 in Physical Chemistry. A Gold Medalist in M.Sc. Chemistry, her current research interests include the investigations of physicochemical interactions at the bio-membrane interface. Her hobbies include reading books



Parteek Prasher

Dr. Parteek Prasher is currently employed as Assistant Professor in the Department of Chemistry, University of Petroleum & Energy Studies, Dehradun. He obtained his M.Sc. Hons. and Ph.D. from Guru Nanak Dev University in medicinal chemistry. His current research interests include bioorthogonal chemistry and therapeutic applications of tailored bioconjugated metal nanoparticles.

sporadic developments and very few candidates with a novel mechanism of action have entered phase II clinical trials over the last two decades.<sup>11</sup> The recent discovery of KAE609 (ref. 12) (1, Fig. 1) and KAF156 (ref. 13) (2, Fig. 1) by Novartis remains the solitary achievement over the past half century. Additionally, the exploration of novel chemotherapeutically operable antimalarial targets,<sup>14a-h</sup> identification of medicinally significant natural products,<sup>15</sup> adoption of polypharmacology,<sup>16a,b</sup> and the utilization of the rational drug designing ‘covalent bi-therapy’ approach<sup>17a,b</sup> have rather reclaimed antimalarial drug discovery.

## 2. Antimalarial chemotherapy

### 2.1 Stages of development of the malarial parasite

Fig. 2 epigrammatically demonstrates the multistage life cycle of the malarial parasite in the vector mosquito and the vertebral host. Each mosquito bite introduces sporozoites into the epidermis.<sup>18</sup> The sporozoites that survive the macrophages reach the hepatic cells of the liver, forming the *liver stage* where they multiply and develop into merozoites.<sup>19</sup> In *P. vivax* and *P. ovale*, the sporozoites may remain dormant for a long time and are termed as hypnozoites, which after a latent period of few weeks or months develop into merozoites.<sup>20</sup> With the rupturing of the matured liver schizont, the merozoites released from the liver enter the erythrocytes, where their population increases profusely, leading to the formation of erythrocytic schizonts *via* a trophozoite stage.<sup>21</sup> This schizont eventually ruptures, releasing the merozoites, which infect fresh erythrocytes.<sup>22</sup> These events comprise the *blood stage* of the malarial parasite, eventually followed by the *transmission stage* where a small proportion of merozoites that do not undergo schizogony differentiate into gametocytes, which are actually non-parasitic and facilitate the generation of zygotes.<sup>23</sup> The zygote may become motile and elongated as ookinetes<sup>24</sup> that invade the midgut wall of the mosquito, thereby developing into oocysts<sup>25</sup> in the last *mosquito stage* of the parasite. The oocysts grow, rupture, and release sporozoites that further expedite the transmission of infection by the female *Anopheles* mosquito.<sup>26,27</sup> Fig. 2 describes the various developmental stages of the malarial parasite.

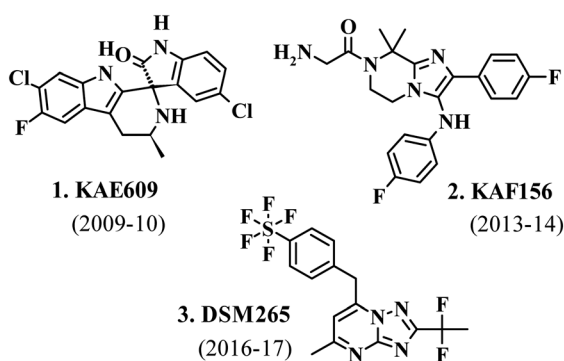


Fig. 1 Recently commercialized antimalarial drugs.

### 2.2 Commercial antimalarial drugs

Table 1 presents a concise summary of the various antimalarial drug classes, the representative drugs therein, and their mechanism of action.

### 2.3 Multidrug resistance in malaria

The first event of MDR malaria occurred in 1950s as chloroquine-resistant *P. falciparum*,<sup>47</sup> following which the parasite reportedly developed resistance to most of the contemporary antimalarial drugs, such as quinine, halofantrine, sulfadoxine/pyrimethamine, and mefloquine.<sup>48</sup> Chloroquine resistance in *P. falciparum* may be multigenic and is primarily offered by point mutations in a gene encoding transporter protein<sup>49</sup> (PfCRT). Reportedly, the efflux pumps of the evolved *P. falciparum* could expel chloroquine 40 to 50 times faster (compared to the sensitive parasite), hence restricting the effective drug concentration for the inhibition of haem polymerization.<sup>50</sup> Conversely, single point mutations in the gene encoding cytochrome B (cytB) in *P. falciparum* confer resistance against atovaquone, often administered in a synergistic combination with proguanil.<sup>51</sup> Moreover, the resistance develops more gradually on combining atovaquone with proguanil or tetracycline than when it is used singly. The resistance in *P. falciparum* against mefloquine and other structurally analogous arylamino alcohols appears due to amplifications in the *Pfmdr* gene encoding for energy dependent p-glycoprotein pump (Pgh).<sup>52</sup> The resistance to antimalarial sulfonamides and sulfones, often administered synergistically with antifolates, appears because of sequential mutations in the *dhps* gene that encodes the target enzyme dihydropteroate synthase.<sup>53</sup> Lately, parasitic resistance has also been reported against artemisinin-based combination therapy and oral artemisinin-based monotherapy (oAMT), hence marring the efficacy of this vital antimalarial class.<sup>54</sup> However, efforts entailing the genome sequencing of *P. falciparum* have validated some potential antimalarial drug targets such as dihydroorotate dehydrogenase enzyme, leading to the identification of clinical drug candidate DSM265 (ref. 55 and 56) (3, Fig. 1) but still, most of the proposed targets identified by genetic knockouts do not comply with chemical validation. The antimalarial drug development regimen, therefore, needs to identify and authorize novel objectives beyond the already well-exploited drug targets. Table 2 presents the characteristic point mutations in the enzymes/proteins that confer MDR to vector mosquito against commercial antimalarial chemotherapy.

## 3. Contemporary antimalarial scaffolds based on the ‘azole’ nucleus

### 3.1 Diazoles

**3.1.1 Imidazoles.** The antimalarial potency of the azoles principally pertains to the inhibition of hemozoin formation.<sup>66</sup> Several azole containing antimycotic drugs such as ketoconazole,<sup>67</sup> miconazole,<sup>68</sup> and clotrimazole<sup>69</sup> (4–6;

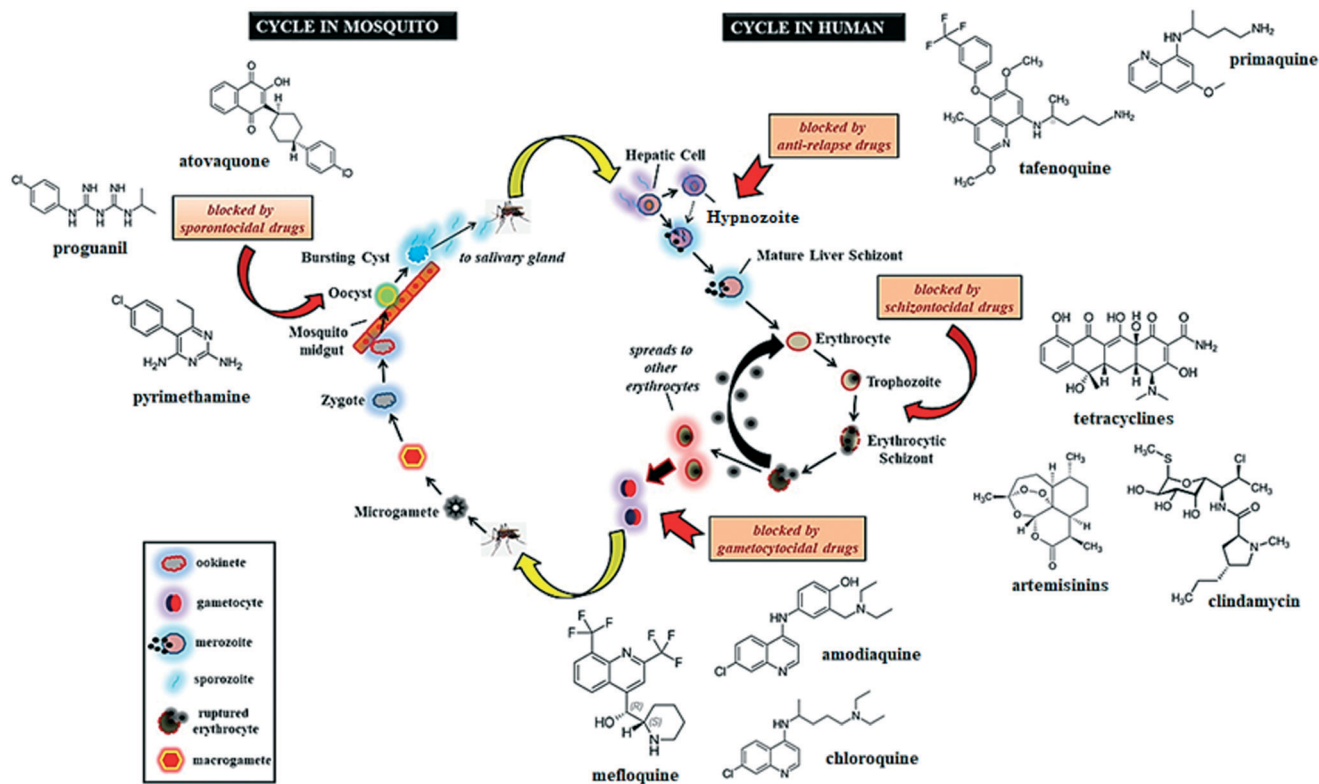


Fig. 2 Life cycle of a typical malarial parasite.

Fig. 3) reportedly inhibit growth in both chloroquine-sensitive and resistant *P. falciparum* with  $IC_{50}$  in the range of 0.2–1.1  $\mu\text{M}$ .<sup>70</sup> The antimalarial effect of ketoconazole appears due to its binding to heme, followed by its removal from both the histidine rich peptide–heme complex as well as the reduced glutathione–heme complex, thereby forming stable heme–azole complexes with two nitrogenous ligands with imidazole nuclei.<sup>71</sup> Conversely, clotrimazole and miconazole exhibit superior antimalarial potency by inducing heme-induced hemolysis.<sup>72</sup> Clotrimazole exhibits high affinity binding for  $\text{Fe}^{3+}$  heme by forming heme–clotrimazole complex that disturbs the degradation of heme GSH.<sup>73</sup> On the other hand, the antimalarial mechanism of ketoconazole and miconazole arises from the inhibition of heme-polymerization and its degradation by GSH and HRP II.<sup>74</sup> Notably, the larger size of the heme–azole complex and hydrophobicity, in addition to the induction of membrane decomposition by this complex, plays a crucial role in the antimalarial action of azoles.<sup>75</sup> Reportedly, the formation of clotrimazole–heme complex averts the conversion of free hemozoin, thereby augmenting the vulnerability of erythrocytes to hypotonic lysis in the presence of heme *via* colloid osmotic hemolysis mechanism.<sup>76</sup> The asexual *P. falciparum* expresses unusual proteins in the invaded erythrocytes that also includes histidine rich proteins (HRPs) containing at least three histidine residues.<sup>77</sup> Reportedly, the localization of HRPs at the outer surface of the erythrocyte membrane as electron-dense knobs creates a highly positive

charge center<sup>78</sup> that facilitates a strong adherence of the infected erythrocytes to the capillary endothelium.<sup>79</sup> HRP1 plays a critical structural and functional role in the survival of the parasite by sequestering the parasitized cells that are otherwise destroyed during their passage through the spleen.<sup>80</sup> Reportedly, 2-fluorohistidine (7, Fig. 3) partially substitutes histidine residues in the *de novo* protein and the 'F' atom moderates the  $pK$  of the imidazole ring from 6 to 1.5, thereby weakening the clusters of positive charge and reducing cellular adherence upon incorporation into the knobs. Notably, at low concentration, 2-fluorohistidine inhibits cyto-adherence and restrains parasitic maturation as well as the appearance of knobs entirely.<sup>81</sup> The antimalarial potency of 2-fluorohistidine led to the further optimization of 2-/5- and 2,5-halogenated histidine, and its decarboxylated analogue histamine (8, Fig. 3). Biological investigations confirmed the inactivity of 5-halohistidine and 2,5-halohistidine as well as 2-chloro and 2-bromo analogues, whereas only 2-iodohistidine displayed antimalarial activity comparable to that of 2-fluorohistidine that reportedly plugs the erythrocyte membrane channels participating in the active/passive transit of essential nutrients required for parasitic survival.<sup>82</sup> However, the metabolic instability of iodine under physiological conditions due to sulfhydryl compounds present in the tissues led to the identification of similarly sized, sterically comparable but metabolically stable molecules such as 1-isopropyl, *tert*-butyl, and benzyl as suitable appendages on histidine (9a–l, Fig. 3) that exhibit a

Table 1 Antimalarial drug classes

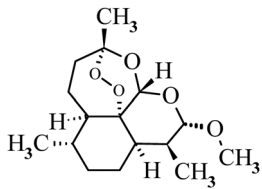
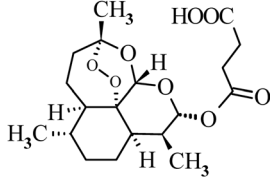
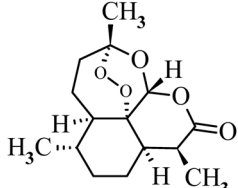
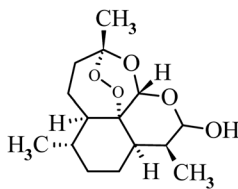
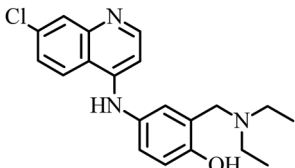
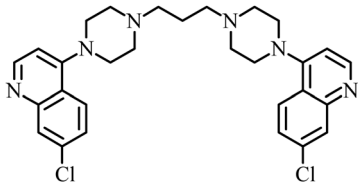
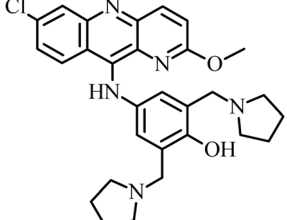
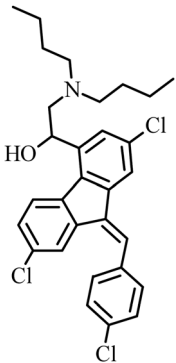
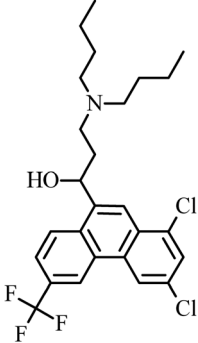
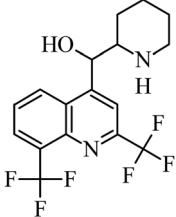
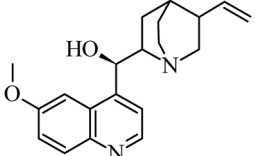
Endoperoxides			
Drug	Target	Structure	Ref.
Artemether	Interacts with ferriprotoporphyrin IX ("heme") in the acidic parasite food vacuole, thereby generating cytotoxic radical species. Also targets the erythrocytic stages of chloroquine-resistant <i>P. falciparum</i> or chloroquine-resistant <i>P. vivax</i> parasites		28
Artesunate	Targets malarial protein EXP-1 and erythrocytic stages of the malaria parasite including the ring stage, late schizonts, and the gametocytes. Restrains cytoadherence by facilitating the splenic clearance of infected erythrocytes. Most potent against <i>P. ovale</i> , <i>P. malariae</i> , and severe <i>P. knowlesi</i>		29
Artemisinin	Targets the histidine-rich protein II (PfHRP II), a recognized heme polymerase, and displaces the heme from PfHRP II, thereby inhibiting heme polymerization and hemozoin formation. Most potent against <i>P. falciparum</i> malaria as well as for chloroquine-resistant <i>P. vivax</i> malaria		30
Dihydroartemisinin	Reportedly binds to haem produced by the parasite's haem biosynthesis pathway (early ring stage) or the haem released by haemoglobin digestion (later stages) in <i>P. falciparum</i> . Another considerable target is the sarcoplasmic reticulum Ca <sup>2+</sup> ATPase pump of <i>P. falciparum</i>		31
4-Aminoquinolines			
Drug	Target/mechanism	Structure	Ref.
Amodiaquine	Inhibits the activity of heme polymerase resulting in the accumulation of free heme that is toxic to <i>P. falciparum</i>		32
Piperaquine	Inhibits the haem detoxification pathway of <i>P. falciparum</i>		33
Pyronaridine	Interferes with the food vacuole of the parasite, targets haematin formation, and reportedly inhibits the decatenation activity of <i>P. falciparum</i> DNA topoisomerase II		34

Table 1 (continued)

4-Aminoquinolines			
Drug	Target/mechanism	Structure	Ref.
Chloroquine	It is active against the erythrocytic forms of <i>P. vivax</i> , <i>P. ovale</i> , and <i>P. malariae</i> , sensitive strains of <i>P. falciparum</i> and gametocytes of <i>P. vivax</i> . Chloroquine reportedly inhibits the parasitic enzyme heme polymerase, which converts the toxic heme into non-toxic hemozoin, thereby resulting in the accumulation of toxic heme in the parasite		35
8-Aminoquinolines			
Drug	Target/mechanism	Structure	Ref.
Primaquine	Generates the reactive oxygen species or by interfering with the electron transport in <i>P. vivax</i> and <i>P. ovale</i> , binds to and alter the properties of protozoal DNA		36
Bulaquine	Damages the parasitic mitochondria, inhibits the protein synthesis, and indirectly inhibits polymerization of amino acids by the plasmodia. Active on <i>P. vivax</i>		37
Tafenoquine	Its active ingredient: 5,6-orthoquinone is redox cycled by <i>P. falciparum</i> , which is further upregulated in the gametocytes and liver stages, producing the ROS that lead to the parasite's death. It also inhibits heme polymerase in the blood stage of the parasite		38
Antifolates			
Drug	Target/mechanism	Structure	Ref.
Pyrimethamine	Inhibits the plasmodial dihydrofolate reductase, thereby impairing the biosynthesis of purines and pyrimidines, thus damaging the DNA synthesis, cell multiplication, and nuclear division at the time of schizont formation in the erythrocytic cycle. Also arrests sporogony in the parasite. Targets <i>P. falciparum</i> and <i>P. vivax</i>		39
Proguanil	It blocks the parasitic dihydrofolate reductase enzyme. Shows synergistic effect with atovaquone in triggering a mitochondrial apoptotic cascade		40
P218	It binds to the active site of <i>P. falciparum</i> DHFR in a highly selective manner and resides almost entirely within the envelope mapped out by the dihydrofolate substrate, which may make it less susceptible to resist mutations		41
Sulfonamide			
Drug	Target/mechanism	Structure	Ref.
Sulfadoxine	Inhibits the enzyme dihydropteroate synthetase, required for converting PABA to folic acid, which is vital to the synthesis, repair, and methylation of DNA and cell growth in <i>P. falciparum</i> . It also targets the parasitic dihydropteroate synthase and dihydrofolate reductase		42

Amino alcohols			
Drug	Target/mechanism	Structure	Ref.
Lumefantrine	It is a blood schizonticide active against the erythrocytic stages of <i>P. falciparum</i> . It inhibits the formation of $\beta$ -hematin by forming a complex with hemin, thereby inhibiting the parasitic nucleic acid and protein synthesis		43
Halofantrine	It is a blood schizonticide, effective against multi drug resistant (including mefloquine resistant) <i>P. falciparum</i> . It acts by forming toxic complexes with ferriprotoporphyrin IX, thereby damaging the parasitic membrane		44
Mefloquine	It is a blood schizonticide, active against the erythrocytic stages of the <i>Plasmodium</i> species resistant to chloroquine. Reportedly, it induces swelling of the <i>P. falciparum</i> food vacuoles by forming toxic complexes with free heme		45
Quinine	It is effective against chloroquine-resistant <i>P. falciparum</i> . It acts as a blood schizonticide and has gametocytocidal activity against <i>P. vivax</i> and <i>P. malariae</i> . Quinine inhibits heme polymerase, thereby allowing accumulation of its cytotoxic substrate, heme. Quinine also interferes with the parasite's ability to break down and digest hemoglobin, and eventually builds up toxic levels of partially degraded hemoglobin in the parasite		46

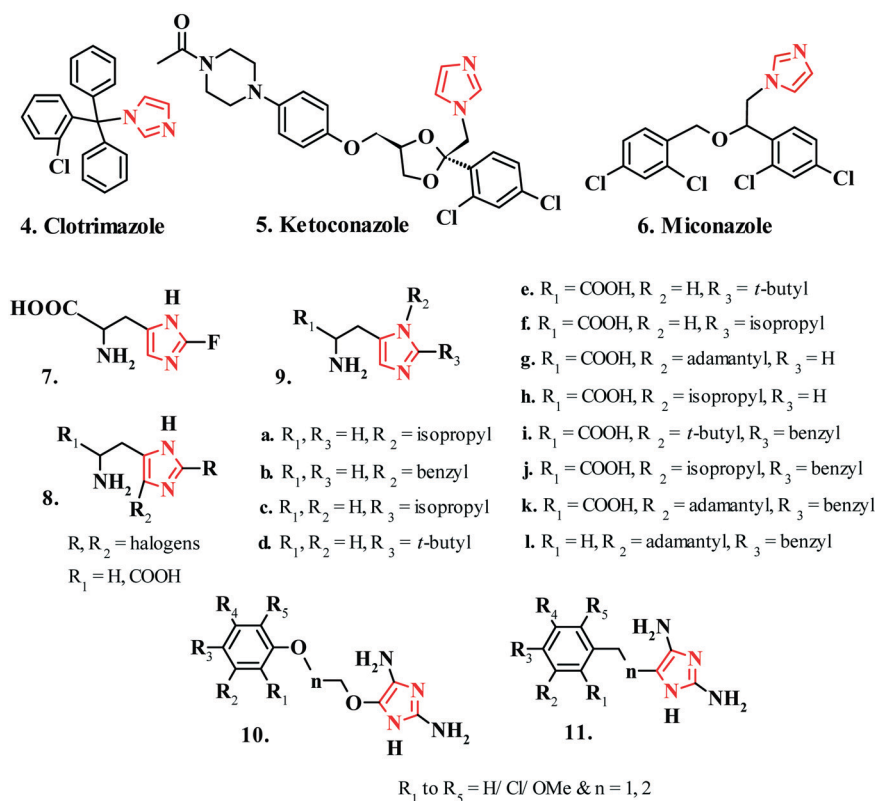
similar mechanism of parasitic inhibition as 2-iodohistidine. These compounds displayed admirable antimalarial activity on chloroquine sensitive and resistant *P. falciparum* strains with  $IC_{50}$  in the range of 10–100  $\mu$ M. Notably, the mono-substituted analogues, specifically at 2-position of both histidine and histamine, displayed the most potent antimalarial activities.<sup>83</sup> Adane *et al.* performed computer-aided molecular design approach involving *ab initio* molecular orbital and density functional theory calculations, along with molecular electrostatic potential analysis and molecular docking studies for optimizing multi-substituted 1*H*-imidazole-2,4-diamines (**10–11**, Fig. 3) as potential inhibitors of *Plasmodium falciparum* dihydrofolate reductase (PfDHFR) enzyme. *In silico* investigations validated the H-bonding interactions of the test compounds with the key amino acid residues such as Asp54, Ileu/Leu164, Asn/Ser108,

and Ile14 present in the active site of the enzyme for promoting the enzymatic inhibition. The candidate compounds displayed a mechanistic similarity with the antifolates. These investigations also played a crucial role in the screening of hit-to-lead molecules as potential inhibitors of wild type and quadruple mutant PfDHFR enzymes. Notably, the flexible appendages in the test compounds prevent non-complementary steric interactions with mutated amino acid residue (*e.g.*, Asn108) in the active site of mutant varieties of PfDHFR enzymes.<sup>84</sup>

**3.1.2 Imidazolidinedione.** The antimalarial screening of imidazolidinedione identified WR182393, a mixture of compounds **12** and **13** (Fig. 4), to be highly efficacious against prophylactic events caused by *Plasmodium cynomolgi*.<sup>85</sup> Guan *et al.* led the structural identification and separation of various bioactive components of WR182393;

**Table 2** MDR conferring mutations in *Plasmodium falciparum*

Gene	Mutation (wild to mutant)	Pathway effected	Drug effected	Ref.
<i>pf dhps</i> 581	Alanine 581 to glycine A581G	Deoxyhypusine synthase	Sulfadoxine	57
<i>pf dhps</i> 540	Lysine 540 to glutamic acid 540E	Deoxyhypusine synthase	Sulfadoxine	58
<i>pf dhps</i> 436	Serine 436 to alanine 436A/phenylalanine 436F	Deoxyhypusine synthase	Sulfadoxine	59
<i>pf dhfr</i> 164	Isoleucine 164 to leucine 164L/methionine 164M	Dihydrofolate reductase	Pyrimethamine	60
<i>pf dhfr</i> 108	Serine to asparagine 108R/threonine 108T	Dihydrofolate reductase	Pyrimethamine	61
<i>pf dhfr</i> 16	Alanine 16 V to serine 108T	Dihydrofolate reductase	Cycloguanil, proguanil	62
<i>pf crt</i> 76	Lysine 164 to threonine 76T	Transporter protein	Chloroquine	63
<i>pf crt</i> 72	Cysteine 72 to serine 72	Chromosome 7	Chloroquine	64
<i>pf mdr1</i>	Asparagine N86 to aspartic acid D1246	Transporter protein	Artemisinin	65

**Fig. 3** 1H-Imidazole based antimalarial scaffolds.

however, poor solubility of the mixture synthesized by the customary protocols challenged the separation and purification, thereby prompting the rational development of novel derivatives of imidazolinedione. Zhang *et al.* reported a first class of chemoprophylaxis antimalarial derivatives (**14**, **15a–j**; Fig. 4)<sup>86</sup> devoid of any activity against blood stage malaria. Notably, these derivatives only targeted prophylactic activity rather than using them directly as treatment therapeutics, thereby resulting in a low parasitic exposure and even lesser chances of appearance of drug resistance in the parasite. The derivatives also exhibited limited oral efficacy in mice infected with sporozoites of *Plasmodium yoelii* and *Plasmodium cynomolgi*, which is a critical parameter in the search for prophylactic drugs. A modest oral activity of these derivatives appeared due to the hydrolysis of the carbamate group by the stomach acid, leading to the

generation of compounds **12** and **13**. The development of novel carboxamide derivatives (**16**, **17a–c**; Fig. 4)<sup>87</sup> overcomes the acid instability of carbamates **14** and **15**. The derivatives **16a–c** displayed a remarkable stability in human and mice liver microsomal preparations. However, the derivatives **17a–c**, being unstable under the same test conditions ( $t_{1/2} < 10$  min), undergo non-enzymatic metabolic transformation to *s*-triazine derivatives at a rapid rate compared to **16a–c**, suggesting that the carboxamides derivatives are prodrugs of *s*-triazine derivatives. Notably, the derivatives **17a–c** displayed superior activity compared to **16a–c** in the exoerythrocytic mouse model but the latter displayed grander prophylactic and radical curative activities in rhesus monkeys. The formation of *s*-triazine, hence, results in chemical inactivation of carboxamide derivatives (**16** and **17**) that offered low activity compared to carbamates (**14** and **15**).

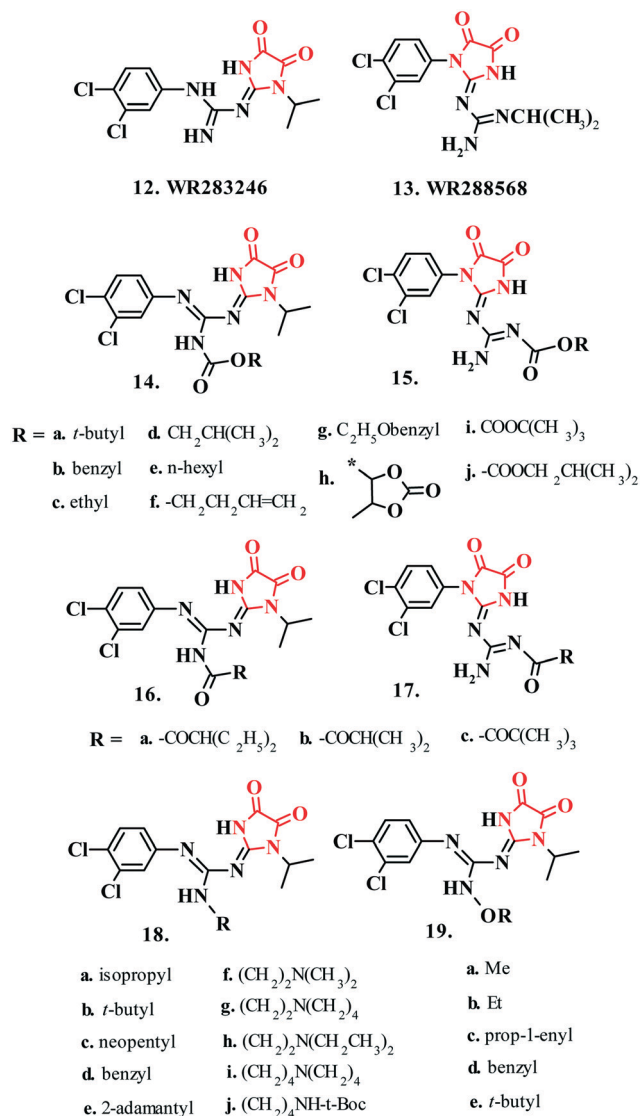


Fig. 4 Imidazolidinedione based antimalarial scaffolds.

Zhang *et al.* designed novel derivatives of *N*-alkyl- and *N*-alkoxy-imidazolidinediones (18a–j, 19a–e; Fig. 4), and evaluated their prophylactic and radical curative activities in mouse and rhesus monkey models. The introduction of *N*-alkoxyl- and *N*-alkyl-functionalities to yield alkylamino- (18a–j, Fig. 4) and alkoxyamine- (19a–e, Fig. 4) derivatives provides chemically stability. The alkoxyamine group is reportedly used as a masking group in the design of amidine pro-drugs.<sup>88</sup> Therefore, its presence in the test derivatives provides an enhanced chemical and/or metabolic stability, resulting in better antimalarial activity compared to the carbamates (14 and 15) and carboxamides (16 and 17). The derivatives displayed metabolic stability with  $t_{1/2} > 60$  min in mice microsomal preparations, however bleak, for *in vitro* activity against *Plasmodium falciparum* clones (D6 and W2) and in mice infected with sporozoites of *Plasmodium berghei*. Notably, the derivatives exhibited substantial prophylactic activity in Rhesus monkeys dosed at 30 mg kg<sup>-1</sup> per day for

three consecutive days compared to the untreated control.<sup>89</sup> Upon oral administration, the derivatives displayed only a fringe bioactivity in causal prophylactic and radical curative tests at 50 mg kg<sup>-1</sup> per day for 3 days and 30 mg kg<sup>-1</sup> per day for 7 days, respectively, in combination with 10 mg kg<sup>-1</sup> chloroquine for 7 days. Importantly, these derivatives exhibited no signs of acute toxicity among the administered mice up to 320 mg kg<sup>-1</sup>.

**3.1.3 Oxoimidazoline.** 4-Oxoimidazoline derivatives (20a–k, 21a–e, and 22a–c, Fig. 5) displayed potent antimalarial activities in rodent and rhesus models. These derivatives demonstrated radical curative activity in non-human primate by the oral route and showed causal prophylactic activity comparable to that of the commonly used clinical drugs in the rhesus model.

In addition, the metabolic profile of the deoxoimidazolidinediones validated their application as prodrugs of the corresponding imidazolidinediones derivatives.<sup>90</sup> Interestingly, the deoxoimidazolidinediones derivatives exhibited only moderate *in vitro* activity against the blood stage malaria, *P. falciparum*, with IC<sub>50</sub> < 1 μg mL<sup>-1</sup>. These derivatives, reportedly, appeared metabolically unstable in the host mice and were metabolized rapidly, thereby yielding hydroxyimidazolinones and imidazolidinediones as the major metabolites. Notably, the isopropyl group with a significant curative effect served as the most potent substituent at R<sub>1</sub> and R<sub>2</sub> of deoxo compounds over the other groups. The rhesus pharmacokinetics data revealed a much longer  $t_{1/2}$  of these derivatives on administration of the drug, likely because of the depot effect of the drug at the injection sites. Additionally, the rhesus pharmacokinetics and the efficacy data held that a lengthier plasma  $t_{1/2}$  of the drug serves as critical factor for regulating its activity against liver stage malaria.

**3.1.4 Imidazoline.** The 5-membered imidazolidinedione ring destabilizes when it carries an electron withdrawing dichlorophenyl substituent. In addition, the presence of two electron withdrawing carboxy groups at 4- and 5-positions of the imidazolidine increases the ring strain, thereby promoting nucleophilic reactions. Zhang *et al.* designed chemically stable imidazoline analogues by replacing the chemically unstable imidazolidinedione ring of the derivatives with a stable imidazoline (23a–e, Fig. 6). These derivatives displayed lower stability in mice microsomal preparation with  $t_{1/2} < 60$  min compared to human microsomal preparation, with a higher rate of drug metabolism in the rhesus microsomal preparation. These compounds also displayed weak to moderate *in vitro* antimalarial activities in three clones of *P. falciparum* (D6, W2, and TM91C235) with IC<sub>50</sub> in the range of 0.2–1.4 μg mL<sup>-1</sup> and protected the mice infected with sporozoites of *P. berghei* at 160 and 320 mg kg<sup>-1</sup> per day by oral dosing.<sup>91</sup>

**3.1.5 Benzimidazole.** Cysteine proteases such as falcipains (FPs) designate unusual therapeutic targets for antimalarial chemotherapy. Confined to the food vacuoles of *P.*



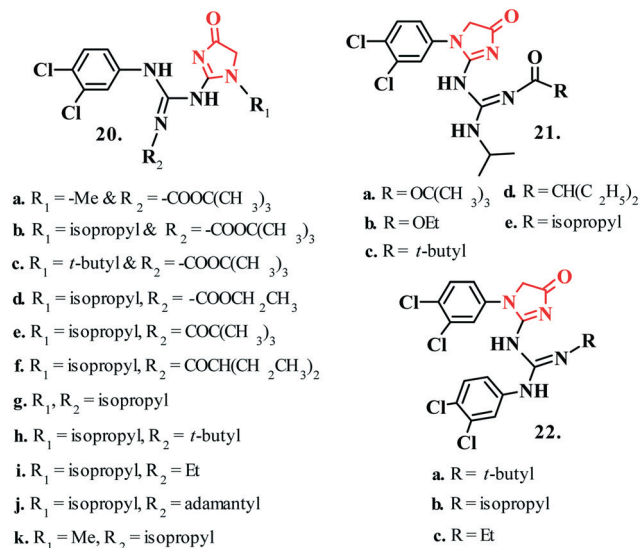


Fig. 5 Oxoimidazoline based antimalarial scaffolds.

*falciparum*, these enzymes play a critical role in parasitic development by degrading the host hemoglobin to the constituent amino acids. However, poor selectivity and considerable toxicity mar the rational development of FPs inhibitors. In addition, the vulnerability of the inhibitors to hydrolysis by host cell proteases also constrains the developmental paradigm. The benzimidazole nucleus readily interacts with tubulin, resulting in the substantial inhibition of the development of malarial parasite. Sharma *et al.* designed non-peptidic inhibitors for FP enzyme by incorporating the benzimidazole moiety anchored with acrylonitriles (**24a–p**, Fig. 7).<sup>92</sup> A considerable heme binding and ferriprotoporphyrin-IX bio-mineralization inhibition along with favorable results in falcipain-2 enzyme assay with  $\text{IC}_{50}$  in the range of 0.69–1.61  $\mu\text{M}$  justified the antimalarial potency of these derivatives. The introduction of intramolecular hydrogen bonding in drug molecules also alters the molecular properties owing to the formation of several conformers that influence the solubility, permeability, pharmacokinetics, and pharmacodynamics, as well as protein binding affinity. The molecules interacting *via* intramolecular H-bonding readily lose water molecules and exhibit lipophilic

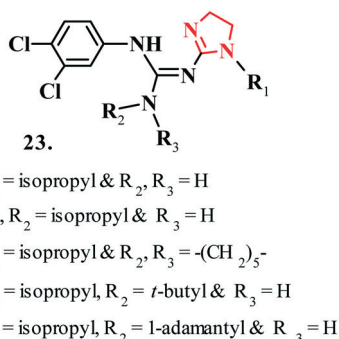


Fig. 6 Imidazoline based antimalarial scaffolds.

interactions while entering a low dielectric environment such as a hydrophobic phospholipid bilayer. Attram *et al.* developed benzimidazole analogues (**25a–l**, Fig. 7) containing an intramolecular H-bonding motif and evaluated the *in vitro* antimalarial activity against chloroquine-sensitive (NF54) and multi-drug resistant (K1) strains of the human malarial parasite *P. falciparum*. The derivatives displayed considerable antiplasmodial (PfNF54) activity with  $\text{IC}_{50} < 1 \mu\text{M}$  owing to the inhibition of hemozoin formation and negligible cytotoxicity. Interestingly, these derivatives displayed intramolecular H-bonding as reflected in the single crystal X-ray analysis.<sup>93</sup> Romero *et al.* developed *N'*-substituted-2-(5-nitroheterocyclic-2-yl)-3*H*-benzo[*d*]imidazole-5-carboxamides (**26a–n**, Fig. 7) as potential inhibitors of  $\beta$ -hematin formation.<sup>94</sup> The *in vivo/vitro* antimalarial investigations on mice infected by a chloroquine sensitive strain of *Plasmodium berghei* ANKA revealed the significant antimalarial potency of these derivatives (upto 98%). Notably, the derivatives enhanced the survival time of mice to an average of  $20.20 \pm 1.95$  days, whereas the progression of infection lowered it to  $3.05 \pm 0.09$ . The test derivatives showed enhanced cytotoxicity against Jurkat E6.1 and HL60 cell lines, whereas fresh human lymphocytes exhibited a negligible effect. Notably, the test derivatives also boosted apoptosis in both the tumor cell lines, thereby lowering cell survival by inhibiting autophagy. Reportedly, the benzimidazole unit participates in  $\pi$ - $\pi$  stacking interaction with the porphyrin ring system. On the contrary, a 5-nitrofuranyl or a 5-nitrothiophen-2-yl substitution on the 2-position and the presence of a phenylcarboxamide appendage in position 5 of the benzimidazole ring, with a replacement pattern of 2, 4 or 3, 4 with lipophilic groups, contributes to an enhanced antiplasmodial activity. Toro *et al.* identified organometallic benzimidazoles as novel scaffolds for developing antimalarial chemotherapeutics. Rationally designed ferrocenyl and cyrhetrenyl benzimidazoles (**27–29**, Fig. 7), and evaluation of their antimalarial properties against the chloroquine susceptible-strain (3D7) and the resistant-strain (W2) of *P. falciparum* revealed that cyrhetrene conjugates present the most potent profile among other organometallic compounds. The presence of  $-\text{NO}_2$  group at the 5-position of organometallic-benzimidazoles augments their antimalarial activity. Interestingly, the biological evaluation against the test strains of *P. falciparum* indicated a superior activity of cyrhetrene conjugates compared to their ferrocenic analogs.<sup>95</sup> Camacho *et al.* designed a new series of *N'*-substituted-2-(5-nitrofuranyl or 5-nitrothiophen-2-yl)-3*H*-benzo[*d*]imidazole-5-carbohydrazide derivatives (**30a–i**, Fig. 7) and investigated them for their potency to inhibit  $\beta$ -hematin formation, hemoglobin hydrolysis, and *in vivo* antimalarial efficacy against *P. berghei*. The derivatives also displayed antitubercular activity against sensitive MTB H37Rv and multi drug resistant MDR-MTB strains.

The derivatives presented favorable activities for the inhibition of  $\beta$ -hematin formation, however, with negligible inhibition of hemoglobin hydrolysis. In addition, these

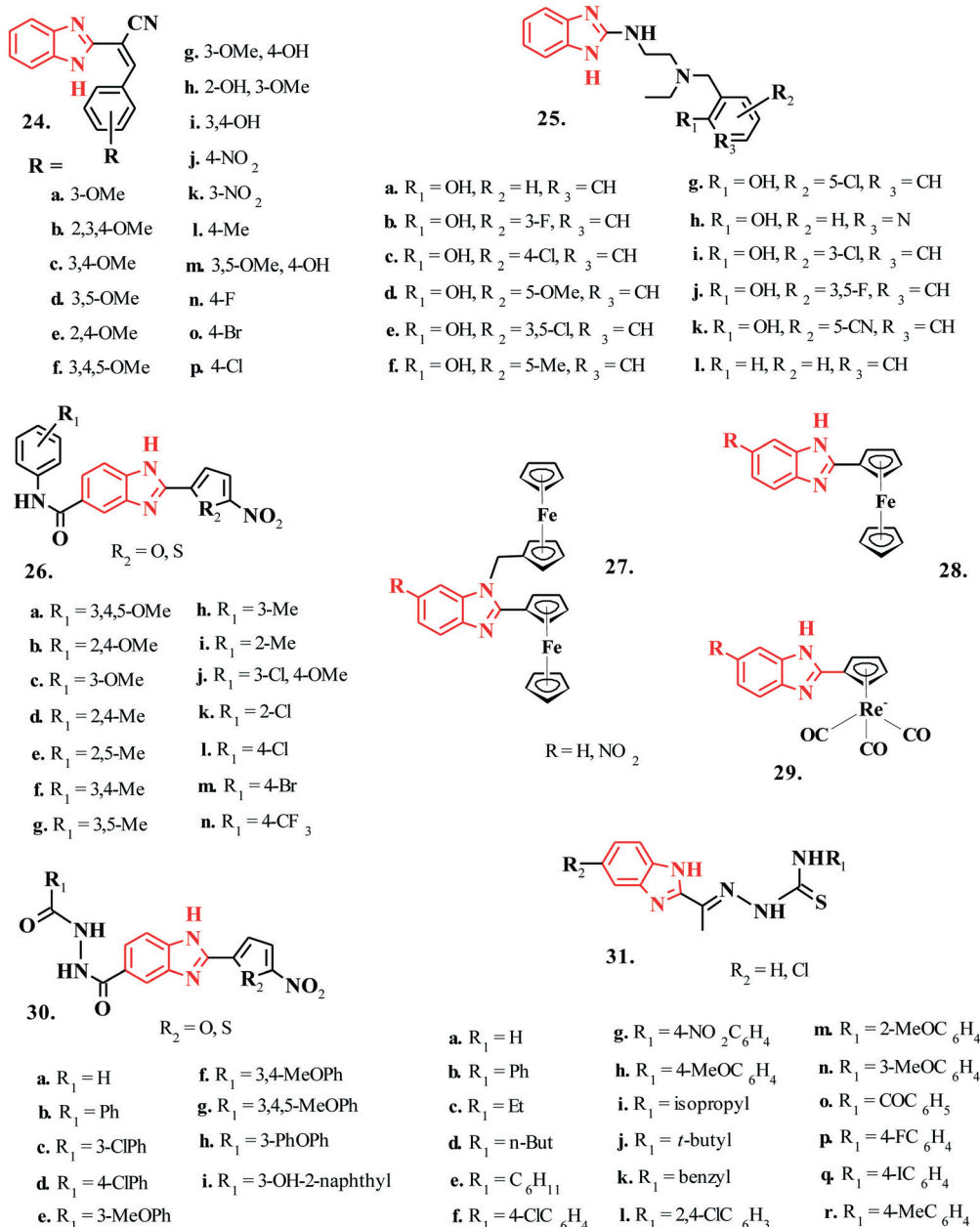


Fig. 7 Benzimidazole based antimalarial scaffolds.

derivatives presented a superior safety index in the *in vivo* cytotoxic investigations against a panel of human tumor cell lines and non-tumorigenic cell lines.<sup>96</sup> Further structural activity relationship (SAR) analysis of benzimidazole was done by Divatia *et al.* by designing (*E*)-2-[5-chloro-1-(1H-benzo[*d*]imidazol-2-yl)ethylidene]-*N*-(substituted)hydrazine carbothioamide derivatives (**31a-r**, Fig. 7) and examining their antimalarial activity.<sup>97</sup> These derivatives inhibited the maturation of the ring stage parasites into trophozoites and schizonts with an IC<sub>50</sub> in the range of 3–54 ng mL<sup>-1</sup>.

**3.1.6 Pyrido[1,2-*a*]benzimidazoles.** Ndakala *et al.* developed a novel class of derivatives based on pyrido[1,2-*a*]benzimidazole scaffold (**32a-r**, Fig. 8) and evaluated their

antiplasmodial activity against drug resistant K1 strain of *P. falciparum*. The most active compound in the library displayed superior *in vitro* activity compared to chloroquine with IC<sub>50</sub> = 0.047 μM. In addition, the antimalarial potency of the derivatives was retained against a spectrum of drug-sensitive and drug-resistant strains, with negligible cytotoxicity against the mammalian (L-6) cell line (selectivity index of >600). Moreover, these derivatives displayed considerable activity in *P. berghei* infected mice following both intraperitoneal and oral administration. Notably, the derivatives displayed >90% inhibition of parasitemia, in addition to an increase in the mean survival time (MSD). However, the pyrido[1,2-*a*]benzimidazoles derivatives

displayed a relatively slower *in vivo* activity as compared to chloroquine. Interestingly, the presence of the alkylamino side chain enhanced the metabolic stability of these derivatives and performed a key function in influencing the *in vivo* activity.<sup>98</sup> Importantly, these compounds display superior stability in rat and mouse microsomes with a long half-life in rats. However, the pharmacokinetic studies indicated that due to their poor solubility, the oral absorption of these compounds becomes saturated at relatively low doses. This necessitates a significant improvement in the pharmacokinetic profile of pyridobenzimidazoles for further development of the lead compounds. Okombo *et al.* further designed a novel library of pyrido[1,2-*a*]benzimidazoles bearing Mannich base side chains (33a-f, Fig. 8) and evaluated them for *in vitro* antiplasmodial activity, microsomal metabolic stability, reactive metabolite (RM) formation, and *in vivo* antimalarial efficacy in a mouse model. The oral administration of active compounds in the library reduced parasitemia by 95% in mice infected with *P. berghei*. Reportedly, the active metabolites of these derivatives contribute to their *in vivo* efficacy. The derivatives reportedly showed rapid metabolism and <40% of the parent compound remained after 30 min of incubation in the liver microsomes. Similarly, RM trapping studies identified glutathione adducts in the derivatives bearing 4-aminophenol moiety, with distinguished fragmentation patterns validating the occurrence of conjugation on the phenyl ring of the Mannich base side chain.<sup>99</sup>

Further structure activity relationship (SAR) analysis on pyrido[1,2-*a*]benzimidazole based antimalarial compounds (34a-t, 35a-l; Fig. 9) identified highly potent and metabolically stable compounds with superior *in vivo* oral efficacy in the mouse infected with *P. berghei*. In addition, the derivatives also displayed potent activity against the liver and gametocyte stages of the malarial parasite with IC<sub>50</sub> in the range of 0.02–0.95 μM and 0.02–1.07 μM against PfNF54

and PfK1 strains. Notably, the inhibition of haemozoin formation qualified as a probable mechanism of antimalarial action.<sup>100</sup> These derivatives displayed swift action (IC<sub>50</sub> (24 h)/IC<sub>50</sub> (72 h) < 1.5), comparable to chloroquine and artemisinin. Notably, the presence of heterocyclic substituents such as hydroxyl pyrrolidine contributed to a significant 3-fold enhancement in selectivity. The introduction of fluoro substituent improved PfNF54 IC<sub>50</sub> by 10–50 times. Similarly, changing the position of –CF<sub>3</sub> from the *para* to *meta*-position did not affect the activity; however, the unsubstituted phenyl along with di-substituted derivatives displayed retention in the activity (PfNF54 IC<sub>50</sub> < 1 μM). Cycloalkyl groups at C-3, including cyclohexyl and cyclopentyl, exhibited minimal cytotoxicity with negligible improvement in the selectivity. Interestingly, the permeability that ranged from moderate to high at pH 6.5, exhibited no interference in the oral absorption of these derivatives from the gastrointestinal tract. On the other hand, the presence of water solubilizing groups such as sulfone did not affect the solubility and proved unfavorable to permeability. Lipophilicity was relatively high for these derivatives (log *P* > 3); however, it promoted enhanced permeability. Nevertheless, these derivatives showed no association between lipophilicity and metabolic stability, thereby validating a greater influence of structural changes on the compound properties compared to physicochemical parameters such as lipophilicity.

**3.1.7 Pyrazoles.** Pyrazoles with a wide range of biological activities act as privileged synthetic inhibitors of several enzymes and biological pathways. Dominguez *et al.* developed a series of substituted pyrazoles (36a-h, Fig. 10) and evaluated their antimalarial activity. Intramolecular H-bonding served as the principal basis of bioactivity of the test compounds. The presence of an ester functionality on the pyrazole ring displayed commendable activity with IC<sub>50</sub> in the range of 0.14–4.6 μmol L<sup>-1</sup>; however, its replacement with a nitrile group resulted in a precipitous loss of activity

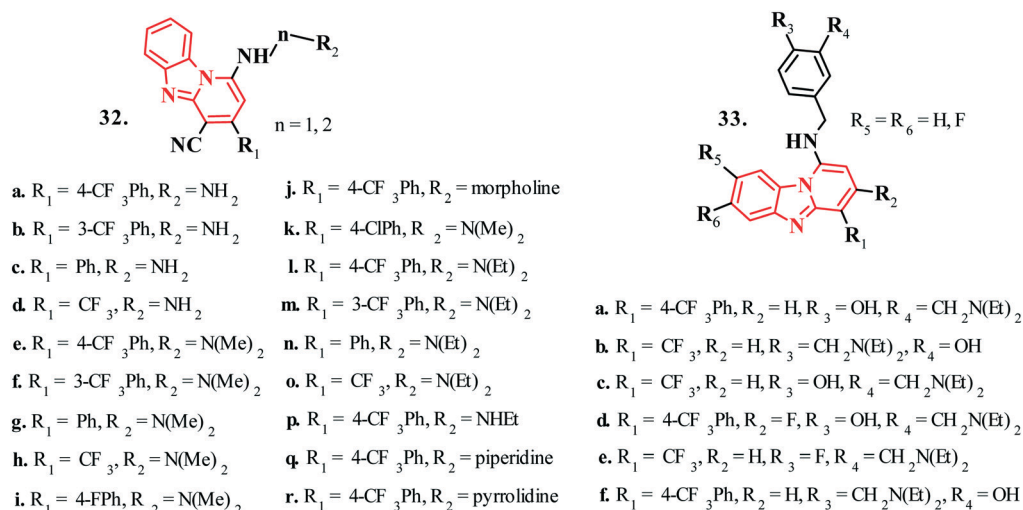


Fig. 8 Pyrido[1,2-*a*]benzimidazole based antimalarial scaffolds contd.

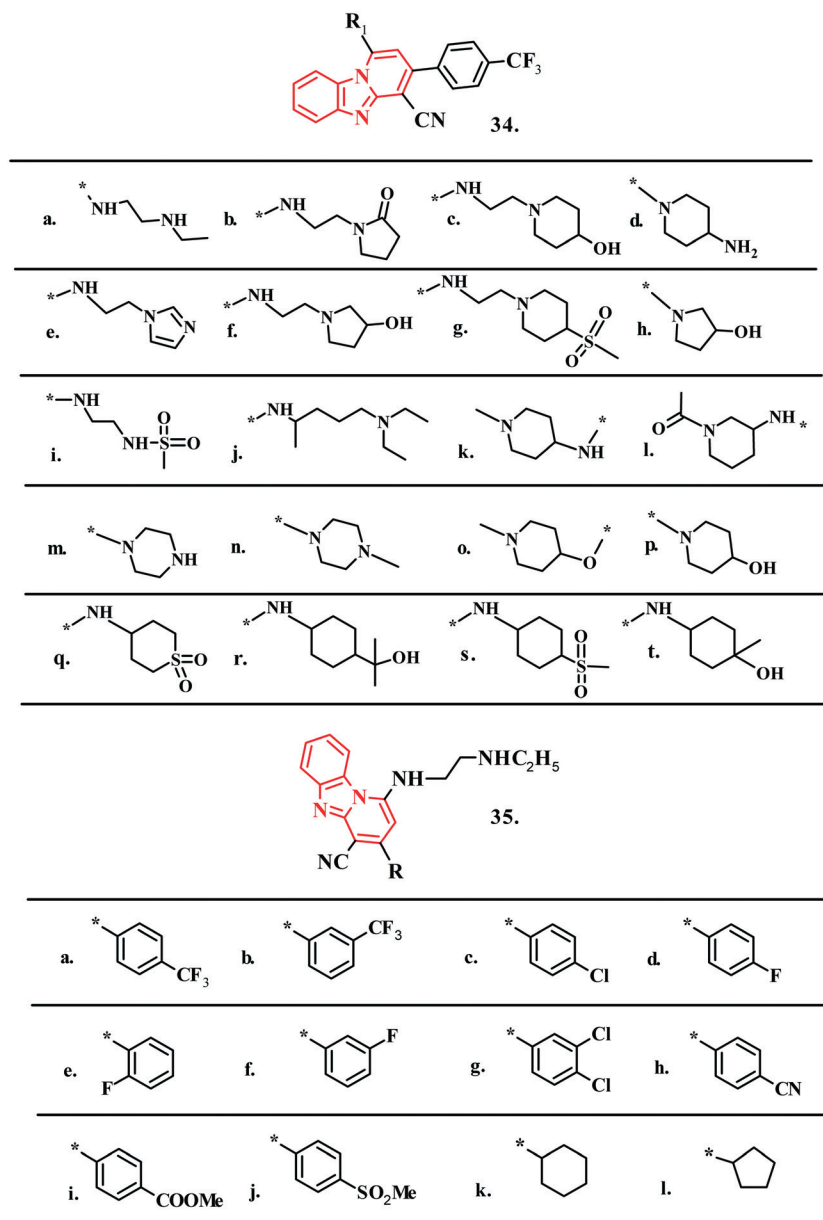


Fig. 9 Pyrido[1,2-*a*]benzimidazole based antimalarial scaffolds.

due to the absence of hydrogen-bond formation.<sup>101</sup> SAR analysis revealed the association of bioactivity caused by electronic effects of various substituents on the phenyl ring present in the compounds. Notably, *meta* substitution augmented the bioactivity whereas *ortho* and *para* substitutions resulted in an eventual loss of antimalarial activity owing to the activation of the *ortho* and *para* positions by moderate electron-releasing groups. Fatty acid biosynthesis (FAS) presents another important targeted pathway in the *P. falciparum* parasite and its human host. The enoyl-ACP (acyl-carrier protein) reductase enzyme (ENR/FabI) catalyzes the concluding reduction step in the final elongation phase of fatty acid synthesis, thereby forming acyl-ACP. The relevance of ENR enzyme in type II dissociative fatty acid synthesis makes it an attractive antimalarial target.

Kumar *et al.* developed a novel series of 1,3- and 1,5-disubstituted pyrazoles (37a–c, 38a–b; Fig. 10) for targeting ENR pathway of *P. falciparum*. The molecules displayed commendable inhibitory potential against enoyl-ACP reductase enzyme with IC<sub>50</sub> in the range of 30–50 μM. The molecular docking experiments on the test compounds indicated extensive binding to the active site amino acid residues of the target enzyme, predominantly *via* hydrogen bonding and aromatic interactions.<sup>102</sup> Bekhit *et al.* reported pyrazole derivatives (39–42, Fig. 10) and evaluated their *in vivo* antimalarial activity in mice models infected with chloroquine sensitive *P. berghei* and chloroquine resistant (RKL9) strain of *P. falciparum*. The reported compounds displayed significant *in vivo* antimalarial activities with mean percent suppression in the range of 83–97% and IC<sub>50</sub> values

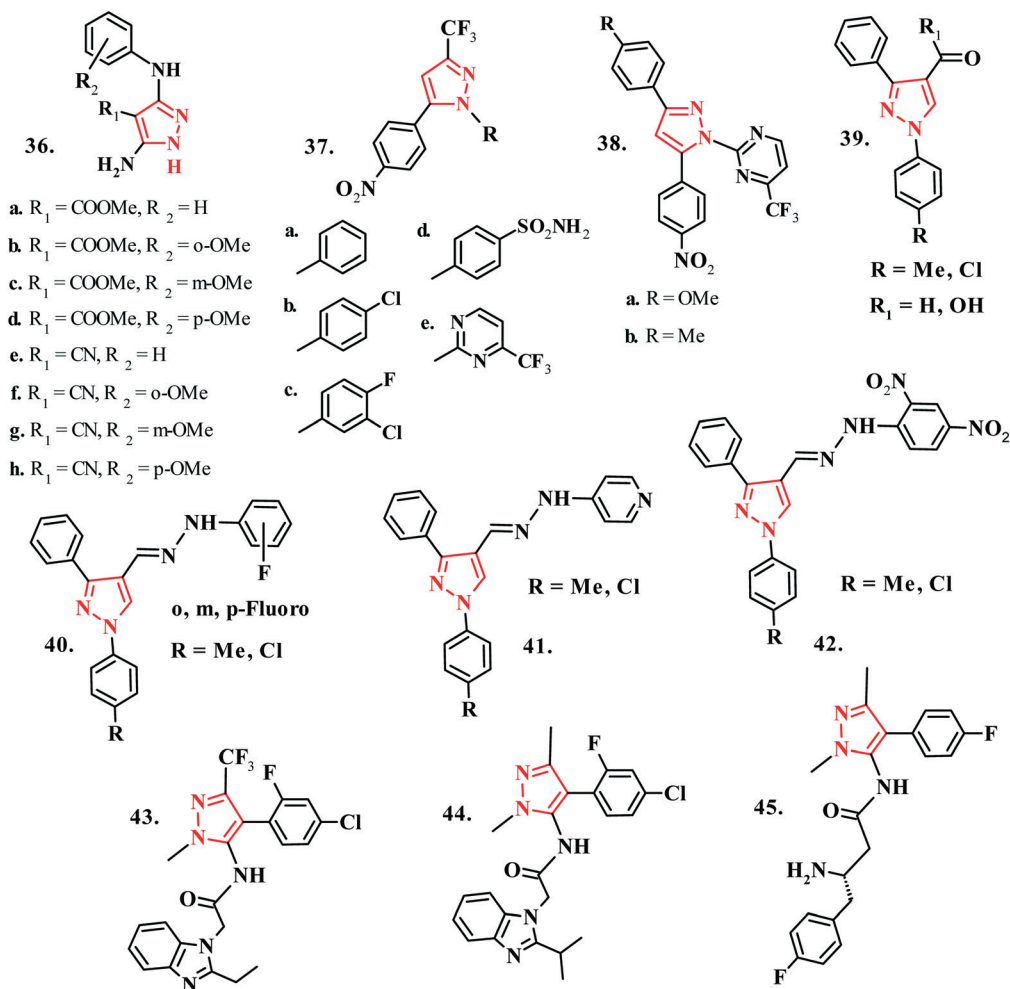


Fig. 10 Pyrazole based antimalarial scaffolds contd.

in the range of 0.033–0.188  $\mu M$  at an equimolar dose level of the standard drug chloroquine diphosphate. Importantly, the acute toxicity studies on the active compounds validated a decent safety profile of these compounds.<sup>103</sup> Vaidya<sup>104</sup> *et al.* identified pyrazoleamides as a novel class of synthetic antimalarial molecules (43–45, Fig. 10) with potent activity against human malarial parasites, displaying a substantial *in vivo* parasite clearance in mice models. The studies involving pyrazoleamide-resistant parasites, whole-genome sequencing, and gene transfer investigations validated that the mutations in two proteins, *viz.*, a calcium-dependent protein kinase (PfCDPK5) and a P-type cation-ATPase (PfATP4), result in the development of full resistance to these test compounds. Reportedly, when the ring-stage parasite advances to the metabolically more active trophozoite stage, it induces a new permeability pathway/plasmodial-surface anion channel in the erythrocyte plasma membrane.<sup>105,106</sup> This event results in increased  $Na^+$  concentration inside the erythrocyte cytoplasm but physiologically low  $Na^+$  levels inside the parasite mediated by a P-type  $Na^+$  ATPase pump encoded by the parasite. These pyrazoleamide derivatives also promote a prompt disruption of  $Na^+$  regulation in blood-

stage *P. falciparum* parasites, exhibiting an effect similar to that of spiroindolones on  $Na^+$  influx in saponin-isolated parasites. Interestingly, merely a 2 hour exposure to the pyrazoleamide compounds led to a significant enhancement in the intact intraerythrocytic trophozoite-stage parasites, eventually leading to dramatic bursting of the parasite. In addition, the efficacy of the test compounds as well as spiroindolones against *P. falciparum* reduced the parasites growing in low  $Na^+$  environment, thereby confirming a common mode of action for these chemically distinct classes of compounds through the disruption of  $Na^+$  homeostasis.

Kumar *et al.* demonstrated the rational design and synthesis of novel acyl hydrazone based molecular hybrids of 1,4-dihydropyridine and pyrazole (46, Fig. 11), and evaluated the *in vitro* antimalarial activities against chloroquine-sensitive malaria parasite *P. falciparum* (3D7). The test compounds displayed superior activity compared to the commercial drug chloroquine and artemisinin with  $IC_{50}$  in the range of 4.40–6.0 nM. The additional *in silico* binding investigations of the test compounds with the enzyme plasmodial cysteine protease falcipain-2 validated systemic inhibition of falcipain-2 as the probable mechanism for the

antimalarial activity.<sup>107</sup> Further, Prasad<sup>108</sup> *et al.* developed imidazo[1,2-*a*]pyrimidine derivatives of pyrazole (47, 48a-g, Fig. 11) and screened these compounds for the *in vitro* antimalarial potency against *P. falciparum* with IC<sub>50</sub> in the range of 0.030–1.45 μg mL<sup>-1</sup>. SAR analysis on the compounds revealed that the presence of imidazole and triazole nuclei at the fifth position of the pyrazole ring in association with varying groups at the *para* position of the phenyl ring and heterocyclic motifs at the sixth position of the pyrimidine ring display susceptibility to incongruent biological activities. The imidazole nucleus in combination with various substituted phenyl and heterocyclic rings in combination compounds with benzylic substitutions (-F, -OH)

demonstrated enhanced bioactivity against the malarial parasite. Conversely, the compounds with -OMe and -Me substituents displayed below average results, whereas in the presence of sulphur and nitrogen containing heterocycles, enhanced antimalarial activity was displayed. Bekhit *et al.* (49–57, Fig. 11) developed 1,3,4-trisubstituted pyrazole derivatives and evaluated their antiplasmodial activity against *P. berghei* and chloroquine resistant strain RKL9 of *P. falciparum*. Most of the derivatives presented a significant percent of inhibition ranging from 90 to 100%. The *in silico* investigations of these derivatives against the wildtype and quadruple mutant pf DHFR-TS structures verified the *in vitro* antimalarial activity. In addition, the derivatives displayed

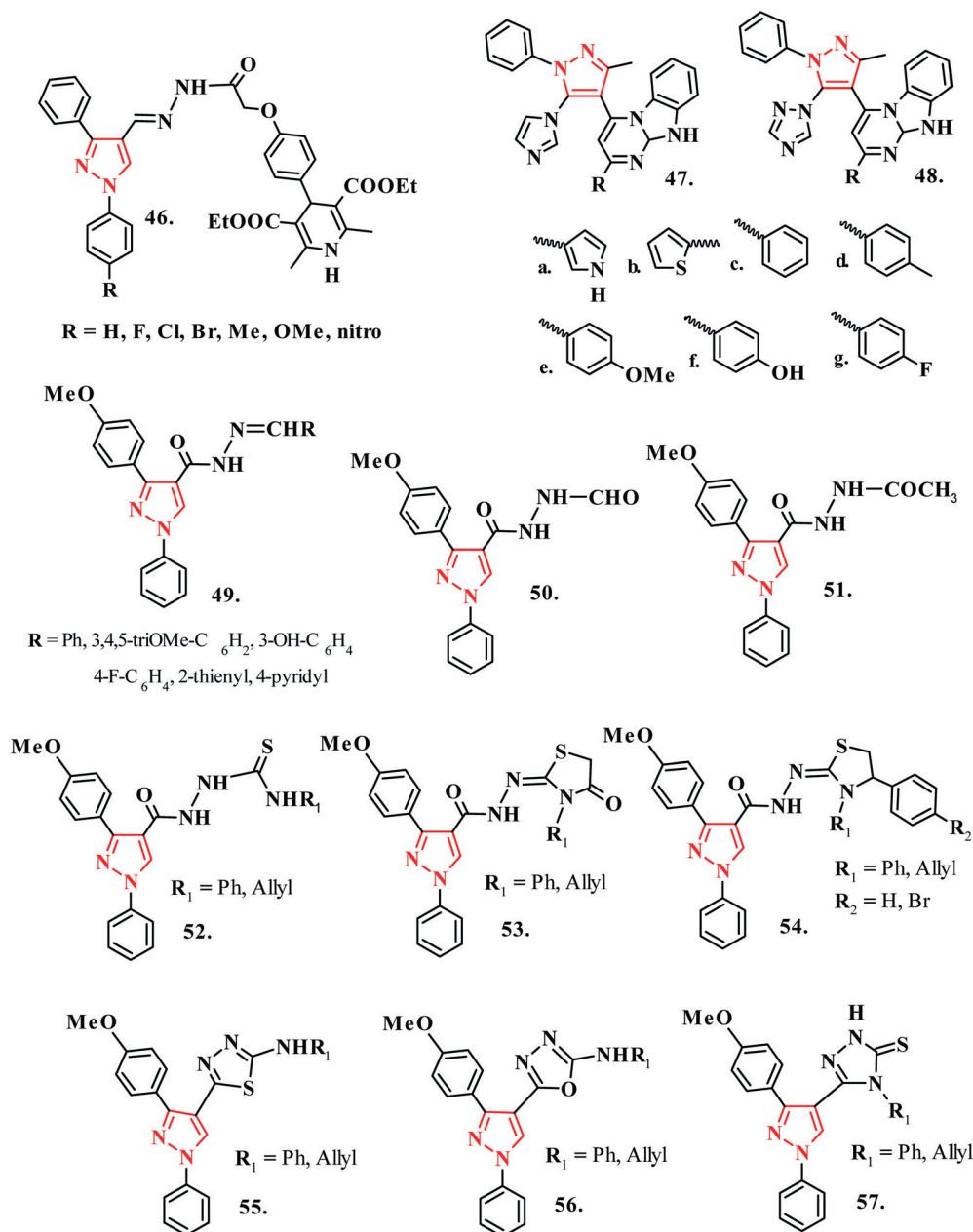


Fig. 11 Pyrazole based antimalarial scaffolds.

substantial *in silico* drug-likeness and pharmacokinetics. Acute toxicity analysis and RBC hemolysis assay revealed sufficient physiological tolerability of the most active compounds up to 150 mg kg<sup>-1</sup> *via* the oral route and 75 mg kg<sup>-1</sup> *via* the parenteral route.<sup>109</sup>

**3.1.8 Imidazole-pyrazole hybrids.** Kalaria and coworkers studied combinatorial libraries of substituted pyrazolines (58, Fig. 12) and isoxazolines (59, Fig. 12) for their *in vitro* antimalarial activity against *P. falciparum*.<sup>110</sup> These derivatives displayed exceptional antimalarial activity with IC<sub>50</sub> in the range of 0.012–0.88 μg mL<sup>-1</sup>. Reportedly, the presence of ‘H’ atom as R<sub>1</sub> and R<sub>2</sub> substituent mainly contributed to the bioactivity of compounds. This further encouraged the development of polyhydroquinoline derivatives<sup>111</sup> (60, Fig. 12) and fused pyran derivatives (61–66, Fig. 12) with an improved activity against the pathogenic *P. falciparum*.<sup>112</sup>

**3.1.9 Pyrazole-pyrazoline hybrids.** Bekhit<sup>113</sup> *et al.* developed pyrazole hybrids with its five-membered bioisostere pyrazoline (67–70, Fig. 13) as potential antimalarial agents in *P. berghei* infected mice and chloroquine resistant (RKL9) strain of *P. falciparum*. These hybrids resulted in >90% suppression of the parasitic activity as compared with the antimalarial reference standard drug, chloroquine phosphate. Importantly, the hybrid compounds displayed admirable safety profile and an oral tolerance up to 300 mg kg<sup>-1</sup> and parenteral tolerance up to 100 mg kg<sup>-1</sup>. Mainly, the hybrids containing ‘NO<sub>2</sub>’ substituent displayed extraordinary antimalarial profile,

superior to the commercial drugs with individual, unhybridized parent scaffolds. Marella *et al.* further developed novel hybrid molecules containing three different scaffolds: pyrazole, pyrazoline, and thiosemicarbazone incorporated into a single compound to get conjugates (71a–t, Fig. 13). The *in vitro* schizontocidal activity against the CQ-sensitive 3D7 strain of *P. falciparum* (IC<sub>50</sub> < 5 μM for most compounds) and cytotoxicity examination against VERO cell lines validated the excellent biological profile of these conjugates. QSAR analysis confirmed that the presence of an electron releasing substituent enhanced the antimalarial activity; however, a hydrogen bond forming electropositive group displayed the most superior activities. The substitution of the electropositive group by an electronegative group leads to diminishing of the bioactivity, with the least activity displayed by the compounds containing electronegative substituents at both the rings B and C on the pyrazole nucleus.<sup>114</sup> The group further developed benzenesulfonamide substituted pyrazole-pyrazoline hybrids (72a–o, Fig. 13) and evaluated the *in vivo* and *in vitro* antimalarial activity against both chloroquine (CQ) sensitive (3D7) and CQ resistant (RKL-9) strains of *P. falciparum*. The derivatives displayed an EC<sub>50</sub> less than 2 μM and acted through the inhibition of β-hematin.<sup>115</sup>

### 3.2 Triazoles

**3.2.1 1,2,3-1H-Triazoles.** Both 1,2,3- and 1,2,4-triazoles present encouraging *in vitro* antiplasmodial and *in vivo*

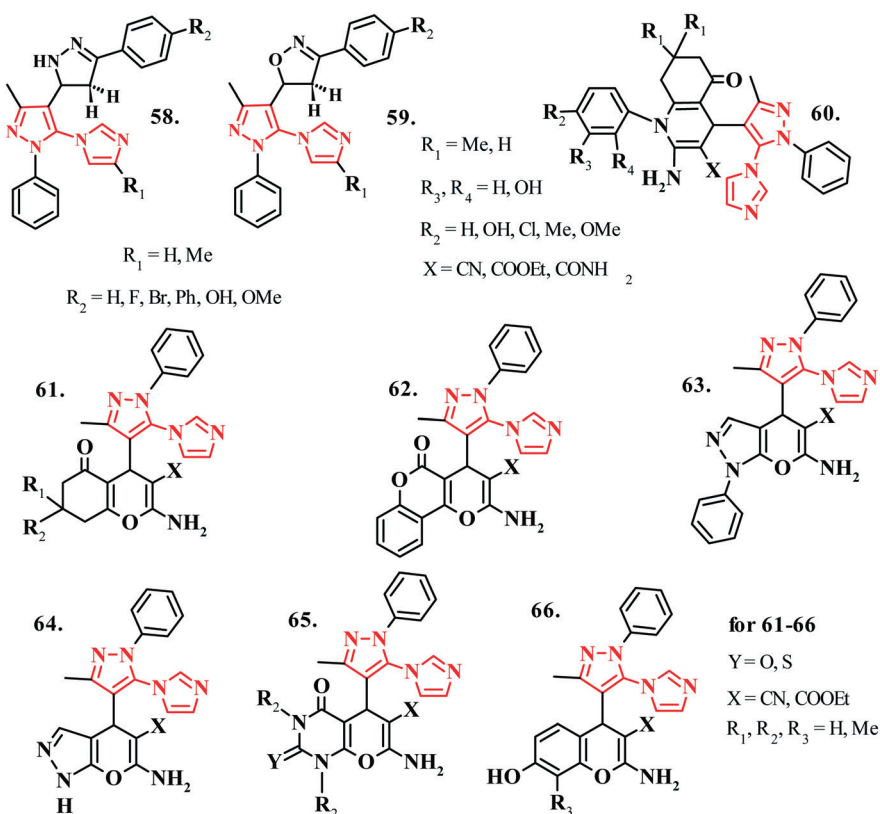


Fig. 12 Hybrid antimalarial compounds based on imidazopyrazole scaffolds.

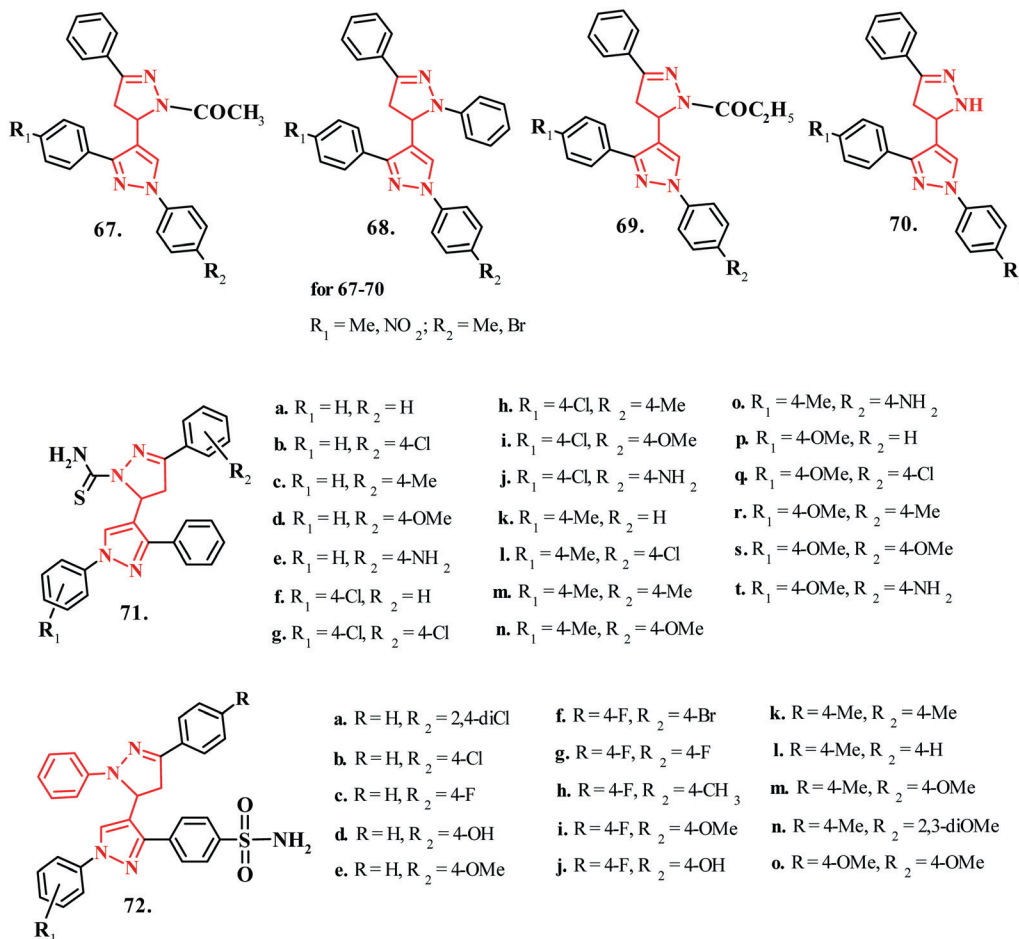


Fig. 13 Hybrid antimalarial compounds based on pyrazole-pyrazoline scaffolds.

antimalarial profile against both the drug resistant and drug sensitive strains. Importantly, the triazole nucleus displays functional isosterism with diverse functionalities such as amide, ester, carboxylic acid, and heterocycles such as pyrazoles,<sup>116</sup> and it employs several non-covalent interactions that improve its solubility and potency to bind to target biomolecules.<sup>117</sup> Interestingly, the hybridization of the triazole nucleus with other synthetic antimalarial pharmacophores delivers novel chemical conjugates expressing admirable biological properties in the current antimalarial paradigm. D' Hooghe *et al.* developed triazole based compounds (73a–e, 74a–e; Fig. 14) showing appreciable antiplasmodial activity against both chloroquine-sensitive and chloroquine-resistant strains with  $\text{IC}_{50} \leq 25 \mu\text{M}$  for majority of the compounds.<sup>118</sup> Balabadra *et al.* developed naphthyl tethered 1,2,3-triazoles (75a–p, 76; Fig. 14) and evaluated *in vitro* antiplasmodial activity against pyrimethamine (Pyr)-sensitive and resistant strains of *P. falciparum* with  $\text{IC}_{50}$  in the range of 19.6–97.5  $\mu\text{M}$ . The acute cytotoxicity analysis of these compounds by employing human embryonic kidney cell line (HEK-293) validated a significant tolerability profile. These compounds curbed the parasitic development and also inhibited the activity of

PfDHFR of the soluble parasite extract. These results supported that the anti-parasitic bioactivity of these compounds appears due to the inhibition of the parasite DHFR as a possible mechanism of action. However, the *in silico* investigations proposed that due to enhanced  $\pi$ - $\pi$  stacking, the bioactivity of these compounds is further enhanced substantially.<sup>119</sup> Patil *et al.* designed aryltriazolylhydroxamates-based histone deacetylase inhibitors (HDACi) with cap group substitution patterns and varying spacer-group chain lengths (77a–j, Fig. 14) that enhance the antimalarial activity. SAR analysis revealed that the anti-protozoan activities of compounds with an unsubstituted phenyl ring depended on the spacer length separating the triazole ring from the zinc binding hydroxamic acid group. Conversely, for the compounds having *N,N*-dimethylamino substitution at the *para* position of the cap group, the antimalarial activity did not depend on the methylene spacer length. Nevertheless, the antimalarial activity of the pyridine-substituted derivatives depended on the ring location of the nitrogen atom. Larger cap groups such as biphenyls, naphthalenes, and quinolines also provided considerable antimalarial activities to the test compounds. Reportedly, the optimized spacer length for the



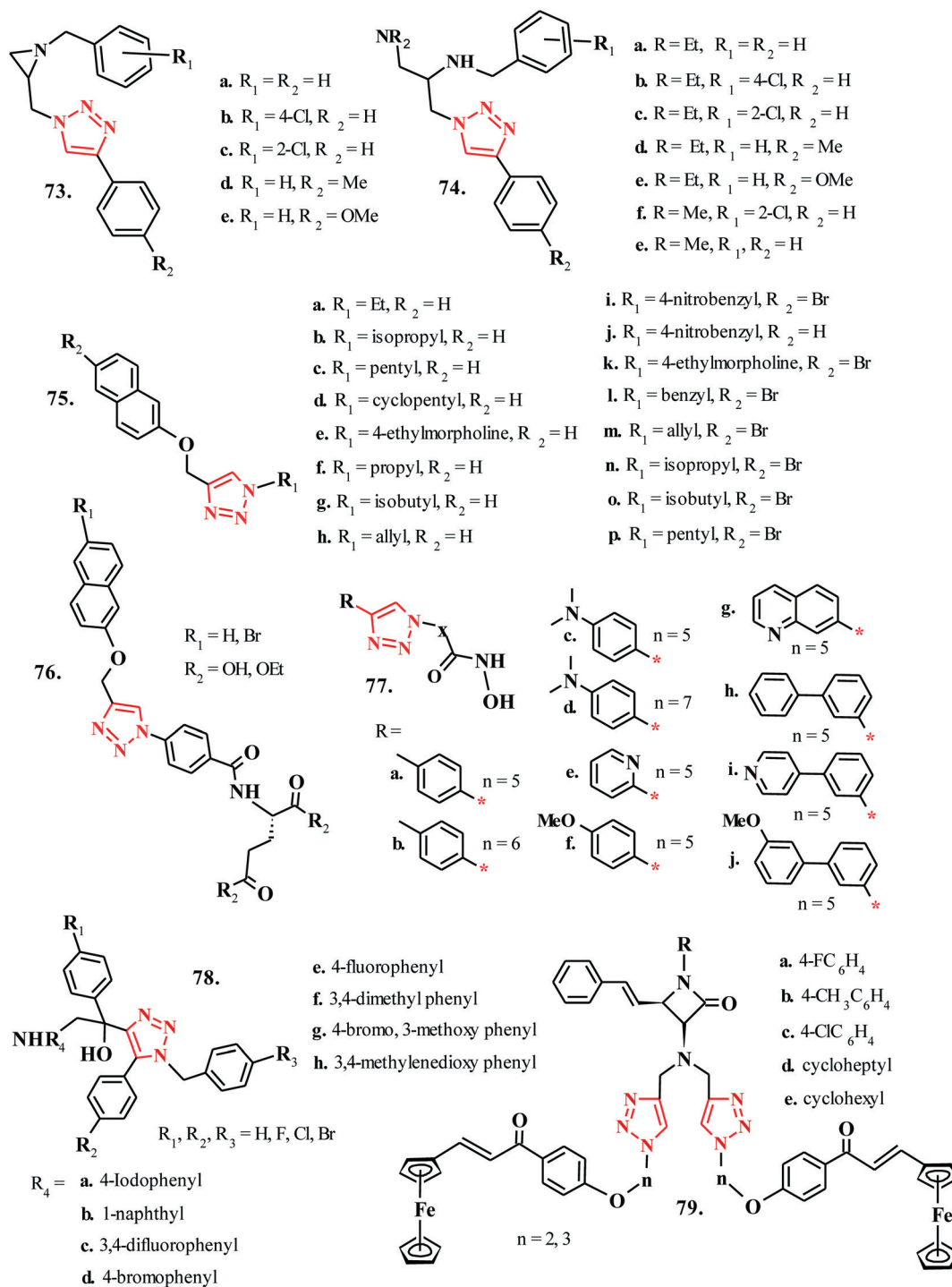


Fig. 14 1,2,3-1H-Triazole based antimalarial scaffolds.

compounds to display anti-parasitic activities was '5' or '6'. Moreover, these compounds potently inhibited the proliferation of the malarial parasite with negligible signs of cytotoxicity to normal mammalian VERO cells compared to the two standard HDAC inhibitors-SAHA and TSA.<sup>120</sup> The validation of a 'triazole' motif in antimalarial drug discovery further prompted the rational development of its hybrid/conjugate compounds.<sup>121</sup> Devender *et al.* synthesized novel

$\beta$ -amino alcohol grafted 1,2,3-triazoles (78a-h, Fig. 14) to evaluate their *in vitro* antiplasmodial and *in vivo* antimalarial activity against chloroquine-sensitive (Pf3D7) strain. The compounds displayed commendable activity with  $\text{IC}_{50}$  in the range of 0.5–0.87  $\mu\text{M}$  compared to the reference drug. The test compounds also displayed significant activity against chloroquine-resistance strain (Pfk1) with >86% inhibition and favorable pharmacokinetic parameters.<sup>122</sup> The

mechanistic evaluations rationalized that the antimalarial activity of the potent compounds appears due to a substantial improvement in the levels of p53 protein, which is reported to lower its levels significantly in the malarial parasite infected hepatocytes.<sup>123</sup> Kumar *et al.* designed ferrocenylchalcone- $\beta$ -lactam hybrids (79a–e, Fig. 14) and evaluated their bioactivity against the chloroquine-sensitive

3D7 and chloroquine-resistant W2 strains of *P. falciparum*. The SAR analysis validated that the N-1 substituent of  $\beta$ -lactam ring decided the bioactivities of these hybrid compounds, being highly potent on resistant strain compared to the sensitive strain. Principally, the compound with *N*-cyclohexyl substituent proved to be the most active and non-cytotoxic with an IC<sub>50</sub> value of 2.36  $\mu$ M against W2

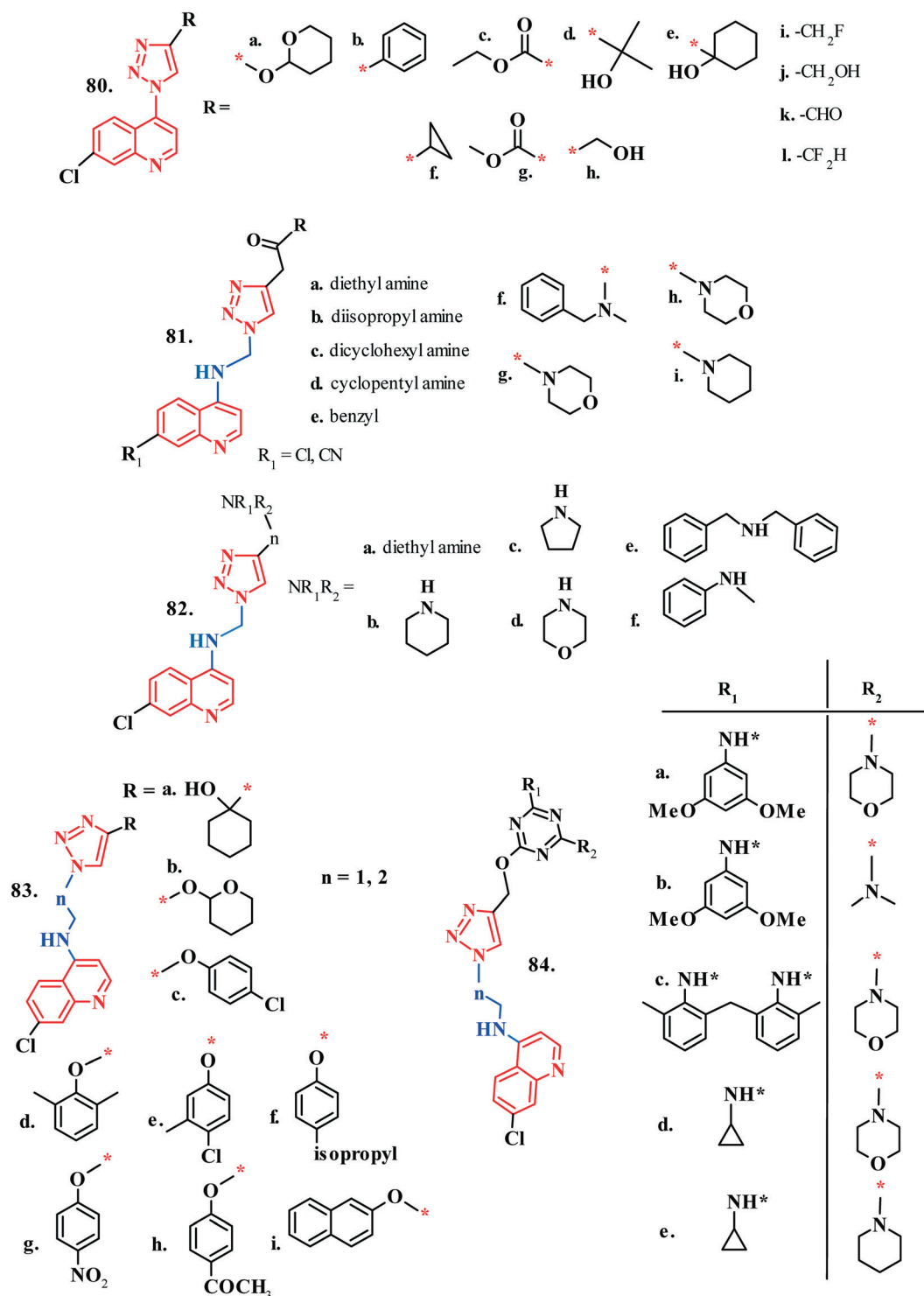


Fig. 15 Hybrid antimalarial compounds based on triazole–quinoline scaffolds.

strain of *P. falciparum*. In addition, the length of the linker and the presence of the bis-ferrocenylchalcones played a secondary role in deciding the antiplasmodial activities.<sup>124</sup>

**3.2.2 Triazole–quinoline hybrids.** Boechat *et al.* developed novel quinoline-1*H*-1,2,3-triazole hybrids (**80a–l**, Fig. 15) with different substituents in the 4-positions of the 1*H*-1,2,3-triazole ring. The *in vitro* investigations of these hybrids on the W2-chloroquine-resistant *P. falciparum* clone exhibited encouraging bioactivity with IC<sub>50</sub> values ranging from 1.4 to 46 μM. These compounds exhibited negligible toxicity to a normal monkey kidney cell-line and presented superior selectivity indexes<sup>125</sup> as high as 351. Further, Joshi *et al.* identified quinoline triazole amide analogues (**81a–i**, Fig. 15) with a 'Cl' and 'CN' substitution at the 7-position of the quinoline ring. These compounds exhibited significant bioactivity against the chloroquine-sensitive D10 and K1 strain of *P. falciparum*, with IC<sub>50</sub> values in the range of 349–1247 nM. The conjugates acted as effective inhibitors of β-haematin, leading to enhanced *in vitro* antimalarial activity. Notably, the hybrids bearing a 'Cl' substituent displayed a resilient linear dependence of log(1/IC<sub>50</sub>) on log*P*, thereby validating an optimum lipophilicity and hence, a superior activity compared to the hybrids with 'CN' substitution. Moreover, a linear dependence on log*P* with a substantially steeper slope for the resistance index (IC<sub>50</sub> K1/IC<sub>50</sub> D10) in the case of the hybrids with 'Cl' substituent revealed the perspectives of producing hydrophilic analogues with strong activity and low cross-resistance with chloroquine.<sup>126</sup> Taleli *et al.* demonstrated *in vitro* antiplasmodial potential of novel triazole-linked chloroquinoline derivatives (**82a–f**, Fig. 15) against NF54 chloroquine-sensitive and Dd2 chloroquine-resistant strains of *P. falciparum* taking chloroquine and artesunate as the reference drugs. Reportedly, these hybrids exhibited a 3–5 fold enhancement in the antiplasmodial activity against chloroquine-resistant strain Dd2 compared to chloroquine with a substantial (>3-fold in comparison to chloroquine) reduction in cross-resistance relative to artesunate.<sup>127</sup>

Manohar *et al.* developed 4-aminoquinoline-1,2,3-triazole (**83a–i**, Fig. 15) and 4-aminoquinoline 1,2,3-triazole-1,3,5-triazine (**84a–e**, Fig. 15) hybrids, and appraised their antimalarial activity against chloroquine-sensitive (D6) and chloroquine-resistant (W2) strains of *P. falciparum*. The structure–activity relationship analysis of these hybrids revealed that simple aliphatic analogues containing polar –OH substituent displayed mild antiplasmodial activity and the protection of –OH group by THP group did not affect the activity. The introduction of an aryl substituent, however, significantly enhanced the activity. Specifically, the aryl groups having halogen and alkyl side chains at various positions of the aromatic ring exhibited similar activities. Interestingly, the presence of –COCH<sub>3</sub> group at *para* position of the aromatic nucleus improved the antimalarial activity against both the test strains, coupled with an increase in the selectivity index. The substitution of the phenyl ring with a biphenyl nucleus also enriched the antimalarial activity. Moreover, the compounds with a C-3 spacer displayed better antimalarial activity compared to their C-2 counterparts due to higher lipophilicity of the compounds with a C-3 spacer. The

introduction of basic moieties such as piperidine, morpholine, and dimethylamine also augments the activity. Similarly, the presence of triazine nucleus with aliphatic moieties diminishes the bioactivity. Importantly, these hybrids displayed non-cytotoxicity up to 48 μM concentration to VERO cells, indicating their tolerance towards mammalian cells. Hence, lipophilicity serves as an important parameter in deciding the antimalarial activity of these hybrids.<sup>128</sup>

**3.2.3 Triazole–chalcone hybrids.** Guantai *et al.* developed a targeted series containing triazole linked chalcone and dienone hybrid compounds containing aminoquinoline and nucleoside templates (**85a–c**, **86a–c**, **87a–e**, **88a–e**, **89a–f**, **90a–f**; Fig. 16) and tested the antimalarial investigations against D10, Dd2, and W2 strains of *P. falciparum*. The dienone based hybrid compounds exhibit below par *in vitro* antimalarial activity relative to their acetylenic precursors. However, the enone–chloroquinoline intermediate compounds displayed superior activities with submicromolar IC<sub>50</sub> values against all the three tested *P. falciparum* strains. Reportedly, the group on the terminal α-carbon of active compounds promotes the retention of activity; however, the presence of halogen functionalities actually refutes the beneficial effects conferred by the chloroquinoline moiety. Also, the presence of α,β-unsaturated carbonyl promotes *in vitro* antimalarial activity. Importantly, the ability of these hybrids to inhibit the formation of β-hematin proposes it to be the primary mechanism of inhibition.<sup>129</sup> The hybrids also exerted negligible cytotoxicity against the Chinese hamster ovarian (mammalian) cell line at the highest concentration tested (100 μM). Kant<sup>130</sup> *et al.* synthesized novel 1,4-disubstituted-1,2,3-triazole derivatives of chalcones and flavones (**91–92**, Fig. 16) and evaluated their preliminary antiplasmodial potential against *P. falciparum* strain 3D7 and human hepato-cellular carcinoma cells (Huh-7).<sup>130</sup> Subsequently, Thillainayagam *et al.* performed molecular docking studies on these hybrids with *P. falciparum* enzyme-dihydroorotate dehydrogenase in order to validate their inhibitory activity against the parasite. The hybrids interact with the active site residues of the target enzyme through numerous hydrogen-bonding interactions with an excellent docking score. Further, evaluations such as molecular dynamic simulations, molecular mechanics/Poisson–Boltzmann surface area free binding energy analysis, and per residue contribution for the binding energy implied that the best-docked *P. falciparum* dihydroorotate dehydrogenase–ligand complex had negative binding energy and affords the most stable, compact, and rigid structure with nine hydrogen bonds.<sup>131</sup> These investigations identified that the compounds with 'F' group at 3- and 'Cl' functionality at the 4-position of the phenyl ring attached to the triazole motif display the most favorable inhibition of the target enzyme.

### 3.3 Tetrazoles

Being a functional bioisostere of –COOH functionality, the tetrazole nucleus can potentially replace carboxylic group in

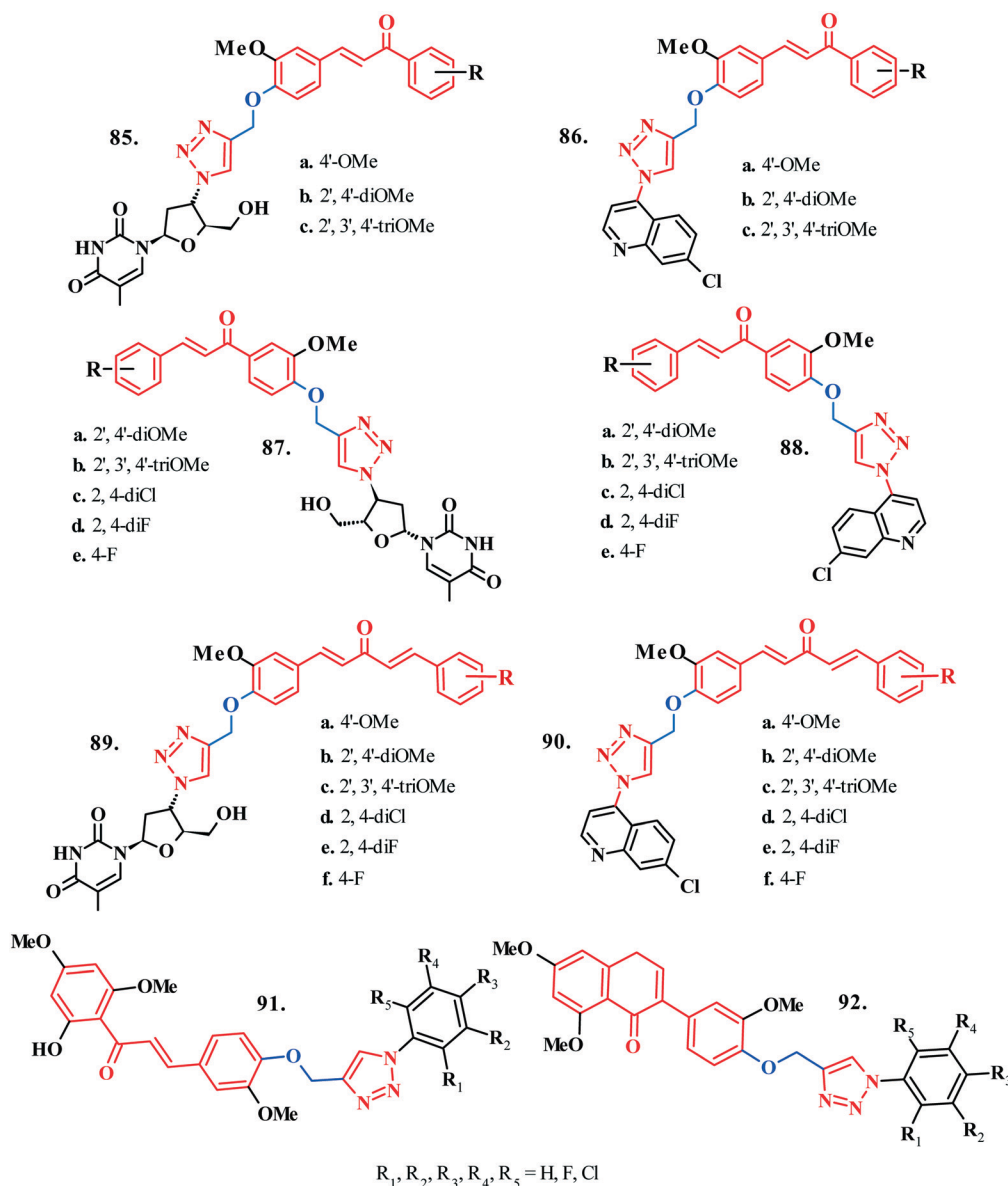


Fig. 16 Hybrid antimalarial compounds based on triazole-chalcone scaffolds.

drugs, thereby improving their lipophilicity, bioavailability, and diminishing the ensuing side effects. In addition, the tetrazole scaffold affords a broad-spectrum of biological properties including antimalarial activities, with several clinically available tetrazole-based compounds for the treatment of various diseases.<sup>132</sup> Interestingly, during the intraerythrocytic stages of the malarial lifecycle, the *Plasmodium* parasites face exposure to heightened fluxes of ROS (reactive oxygen species), principally based on the glutathione reductases of the malarial parasite *P. falciparum* and the host erythrocyte. Biot *et al.* utilized menadione chemistry to screen tetrazole based hybrids (**93**, Fig. 17) as inhibitors of the parasitic enzyme glutathione reductase. The hybrids with 'CN' functionality showed improved antiplasmodial activity with improved bioavailability.<sup>133</sup> Tukulula *et al.* developed a novel series of

deoxyamodiaquine-tetrazole hybrids and evaluated them *in vitro* for antiplasmodial activity against chloroquine resistant K1- and W2-strains of *P. falciparum*. The *in vitro* ADME characterization of the active compounds indicates rapid metabolism with a higher rate of clearance in human and rat liver microsomes. The identification of metabolites by the LC-MS method suggested the metabolic lability of the groups attached to the tertiary nitrogen. Furthermore, the preliminary studies on these hybrids and *in silico* investigations rationalized their strong inhibitory potential against major CYP450 enzymes<sup>134</sup> (**94**, Fig. 17). Pandey *et al.* procured novel tetrazole hybrids appended to 4-aminoquinoline (**95–101**, Fig. 17) and screened their antimalarial activities against both chloroquine-sensitive (3D7) and chloroquine-resistant (K1) strains of *P. falciparum* as well as for cytotoxicity against VERO cell lines. The hybrids

exhibited potent antimalarial activity as compared to chloroquine against the test K1-strain.

In addition, the active hybrid compounds during their *in vivo* investigations on Swiss mice infected with *P. yoelii*, following both intraperitoneal and oral administration, showed a significant 99.99% suppression of parasitaemia after 96 hours of administration.<sup>135</sup> Lobo *et al.* designed endoperoxide-derived compounds, with trioxolane (ozonide) or a tetraoxane moiety, flanked by adamantane and a substituted cyclohexyl ring appended at one end, and a substituted tetrazole nucleus flanked at the other end (102–104, Fig. 17). These hybrids exhibited sub-micromolar antimalarial activity in the range of 0.3–71.1 nM, with negligible cross-resistance with artemisinin or quinolone derivatives. Importantly, the hybrids also displayed insignificant cytotoxicity towards the mammalian cells.<sup>136</sup>

### 3.4 Thiazoles

Thiazoles represent a privileged heterocyclic scaffold with diverse biological properties for curing several infectious

diseases.<sup>137</sup> Karade *et al.* procured a novel series of thiazole-derived *N*-Boc amino acids derivatives (105a–h, 106a–b; Fig. 18) and evaluated their potential antimalarial potency against plasmepsins II enzyme of malaria parasite *P. falciparum*. These derivatives displayed commendable bioactivities with IC<sub>50</sub> values in the range of 3.45–4.89 μM. Moreover, the molecular docking investigations of these hybrids in the active site of plasmepsin II revealed their interaction with the active site residues ASP34 and ASP214, with a significant correlation between the binding energy and the antiparasitic activity of these compounds.<sup>138</sup> Bueno *et al.* synthesized a series of thiazole analogs (107, Fig. 18) and performed SAR analysis for their *in vitro* activities against the 3D7 strain of chloroquine-sensitive *P. falciparum*. Reportedly, the adjustments of the *N*-aryl amide group appended to the thiazole nucleus play a crucial role in deciding the *in vitro* antimalarial activity and cytotoxicity of these compounds. The investigations claimed that non-bulky, electron-withdrawing groups at the *ortho* position on the phenyl ring significantly enhance the bioactivity; conversely, small atoms such as H and F improve the activity when present at the

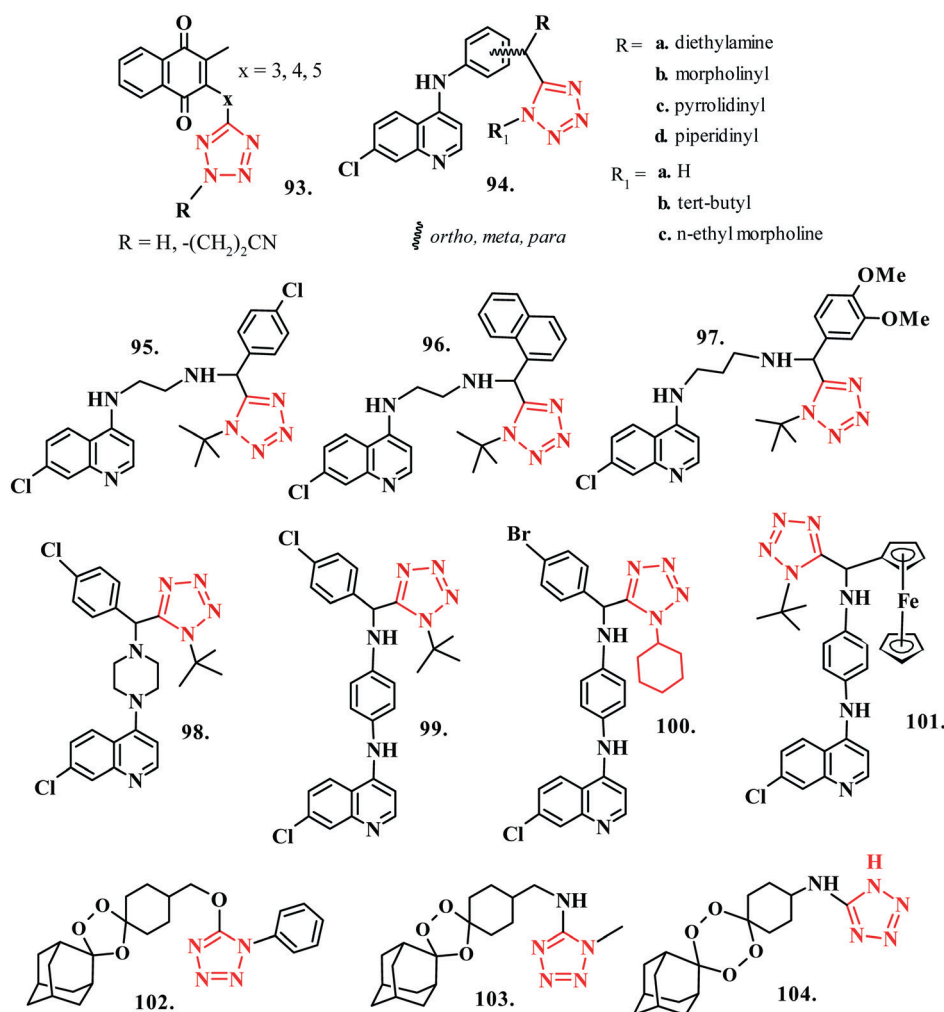


Fig. 17 Tetrazole based antimalarial scaffolds.

*para* position. In addition, the substitution of the phenyl ring by a pyridine nucleus improves the physicochemical properties without compromising the *in vitro* bioactivity. Due to the presence of amino acids, these compounds displayed mild cytotoxicity against HepG2 human liver cells.<sup>139</sup> Makam *et al.* reported SAR analysis on novel 2-(2-hydrazinyl)thiazole derivatives (**108a-r**, Fig. 18) and examined their antiplasmodial activity against NF54 strain of *P. falciparum* by *in vitro* blood stage assay. The derivatives showed substantial antimalarial potency with significant binding interactions with *trans*-2-enoyl acyl carrier-protein reductase of *P. falciparum*, as studied through molecular docking

investigations. The IC<sub>50</sub> for these compounds was in the range of 0.725–631.84 μM. The analysis also revealed the importance of the 2-pyridyl system in the contemporary antimalarial paradigm that follows the inhibition of PfENR protein pathway to kill *P. falciparum*.<sup>140</sup> *Plasmodium* cyclic GMP-dependent protein kinase (PKG) represents a key pathway in the erythrocytic stages of development of *P. falciparum*, as well as in liver stage development.<sup>141</sup> Penzo *et al.* studied the potential of thiazoles for targeting PfPKG11 and PfPKG38. The representative compounds (**109–111**, Fig. 18) showed a substantial inhibition of the target enzyme coupled with the deactivation of additional kinases. In

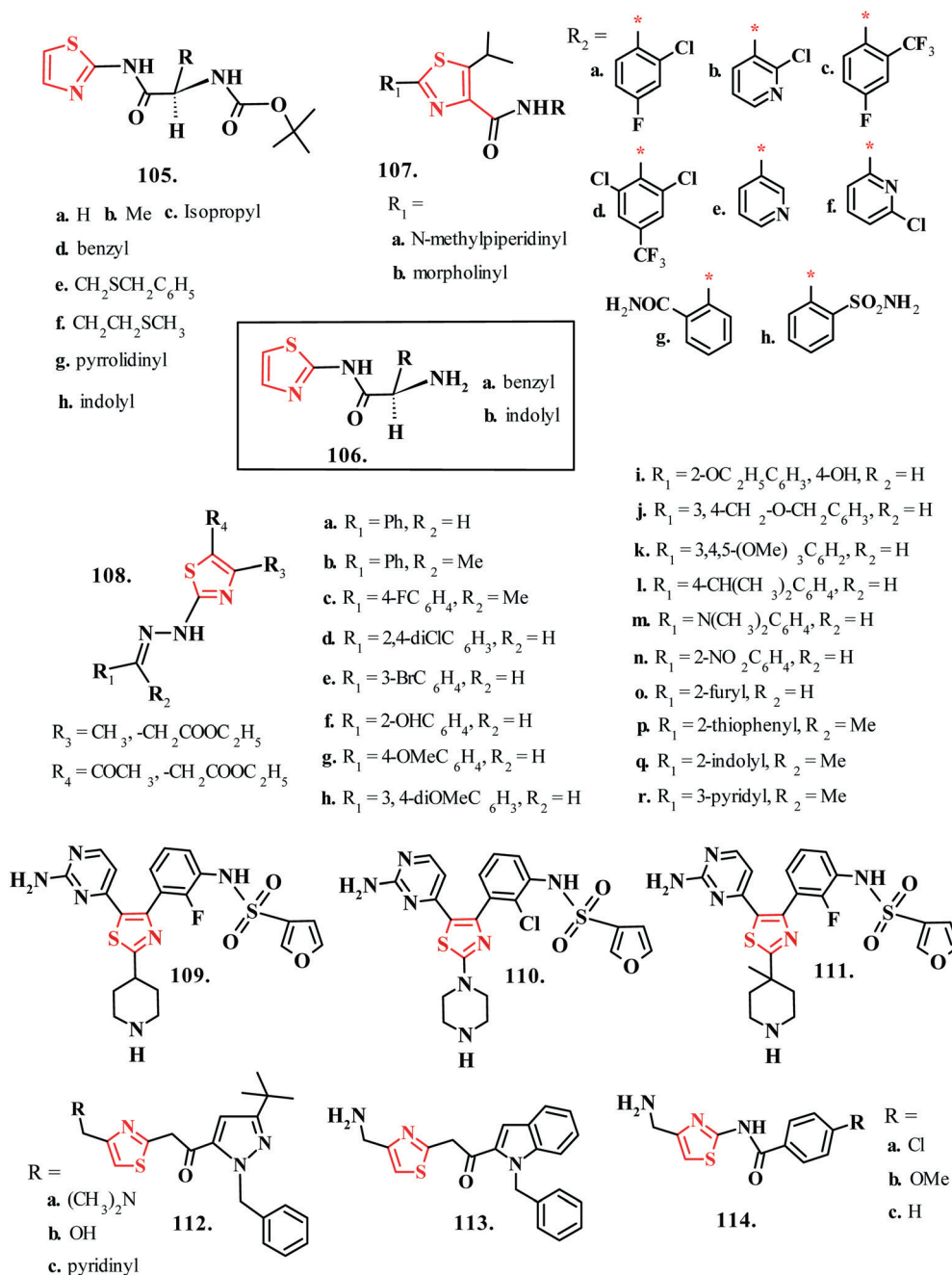


Fig. 18 Thiazole based antimalarial scaffolds.

addition, these compounds displayed nanomolar inhibitory concentration against blood stages and nanomolar to low micromolar potency against male and female gametocytes.<sup>142</sup> Cabrera<sup>143</sup> *et al.* developed a novel library of aminomethylthiazole pyrazole carboxamides derivatives (**112a-c**, **113**, **114a-c**; Fig. 18) offering superior *in vitro* activity against K1 and NF54 strains of *P. falciparum* with improved oral efficacy and pharmacokinetic profile in a *P. berghei* mouse model. The most potent compounds in the library presented better stability in the rat and mouse microsome with a considerably lengthier half-life (>3 h) in rats. In addition to a low cytotoxicity profile, the pharmacokinetic

investigations validated a decent oral bioavailability (51% at 22 mg kg<sup>-1</sup>). Importantly, these compounds also offered modest absorption rate with high volume of distribution with a moderately high plasma and blood clearance.<sup>143</sup>

**3.4.1 Benzothiazole.** Benzothiazole reportedly acts as a functional bioisostere of quinoline, thereby supplementing the antimalarial activities of the latter to the former.<sup>144</sup> Burger *et al.* studied the SAR of 2,6-disubstituted benzothiazole derivatives appended with amino alcohols and a phenyl/trifluoromethyl functionality (**115a-r**, **116a-c**; Fig. 19). The appraisal of their antiplasmodial activity against *P. berghei* infected mouse models revealed a mild bioactivity;

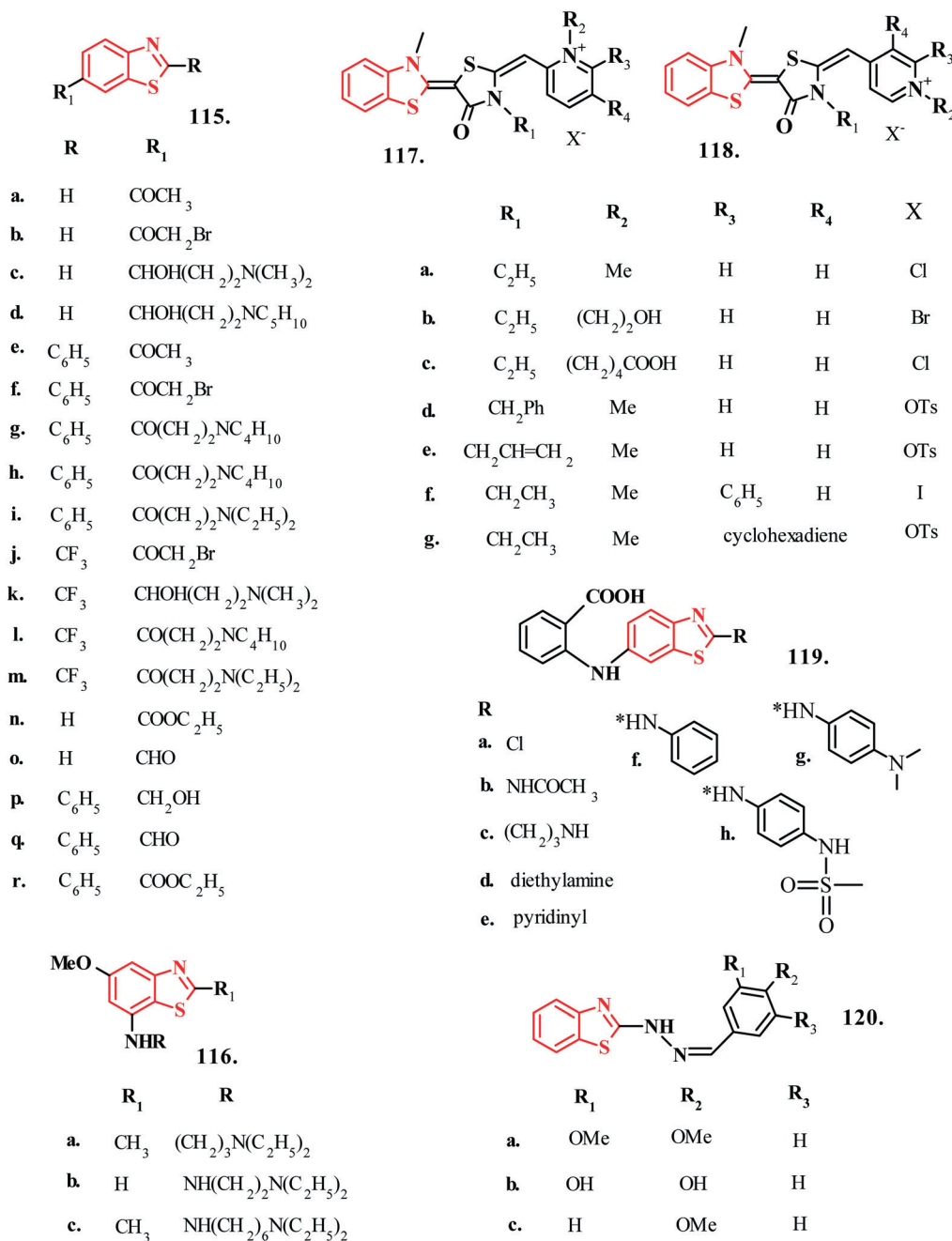


Fig. 19 Benzothiazole based antimalarial scaffolds contd.

however, it recognized the relevance of benzothiazole nucleus in developing antimalarial chemotherapeutics.<sup>145,146</sup> Takasu *et al.* further extended the research on benzothiazole based antimalarial compounds by reporting rhodacyanine derivatives containing benzothiazole (117a–g, 118a–g; Fig. 19) nucleus containing a variety of linked heterocyclic moieties that possess superior *in vitro* activity against *P. falciparum* coupled with low cytotoxicity.<sup>147</sup> The *in vitro* EC<sub>50</sub> values of these derivatives against *P. falciparum* was in the range of 4–300 nM with an outstanding selective toxicity profile (>100). These investigations further validated the position of the

benzothiazole moiety in the development of antimalarial chemotherapeutics. Hout *et al.* tested the antiplasmodial efficacy of 2-substituted 6-nitro- and 6-amino-benzothiazoles (119a–h, Fig. 19) by performing *in vitro* investigations on W2 and 3D7 strains of *P. falciparum* and clinical isolates from malaria-infected patients, in addition to the acute cytotoxicity investigations on THP1 human monocytic cells. The *in vivo* investigations on *P. berghei*-infected mice and *in vitro* investigations revealed the bioactivity of these compounds on all stages of the parasite; however, the principal mechanism of inhibition occurred by impairing the mature schizont

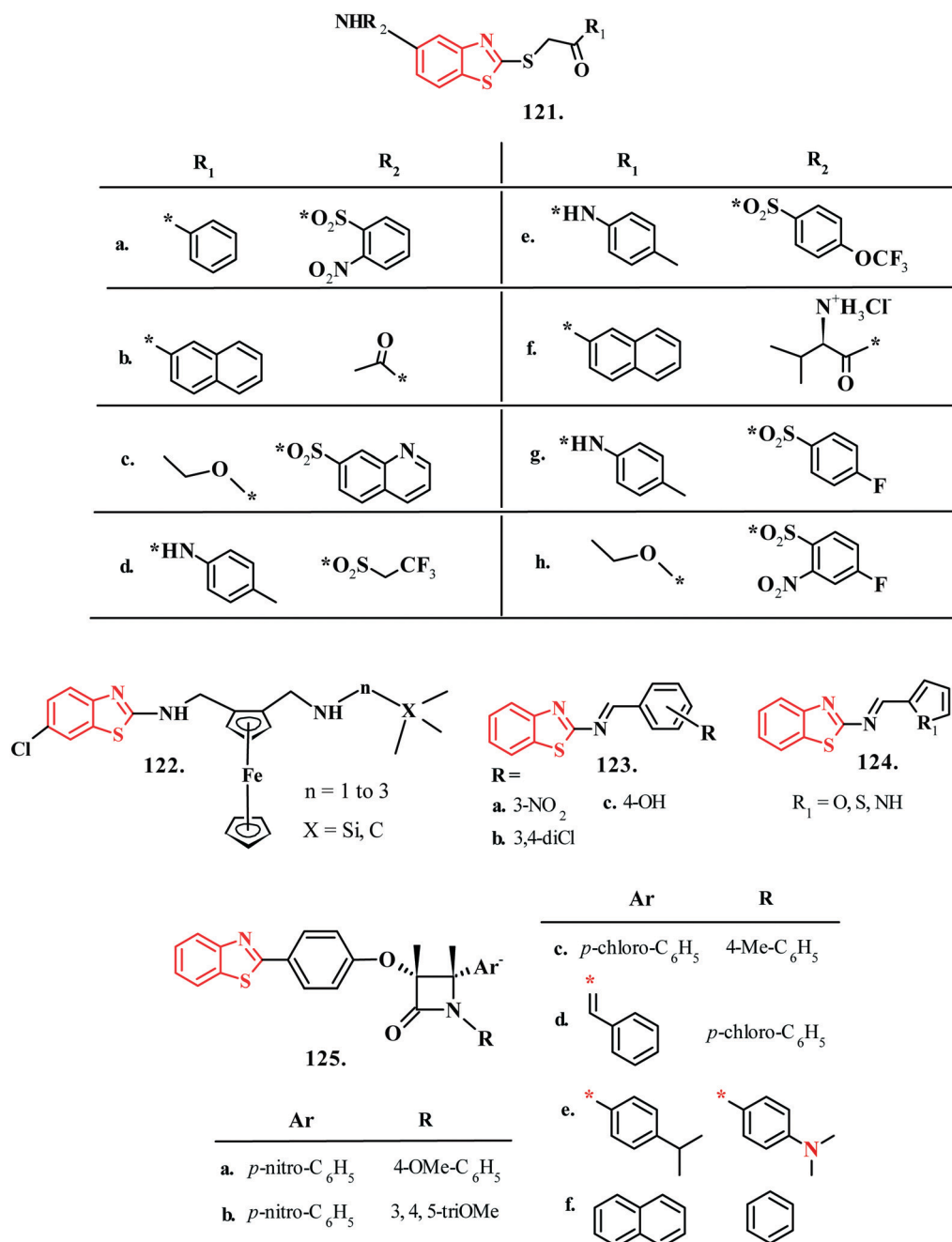


Fig. 20 Benzothiazole based antimalarial scaffolds.



stage as well as the young schizont forms. The *in vivo* data confirmed the efficiency of these compounds with a persistent reduction in parasitaemia.<sup>148</sup>

Sarkar *et al.* synthesized benzothiazole-hydrazone conjugates (**120a–c**, Fig. 19) and tested *in vitro* and *in vivo* activity against chloroquine/pyrimethamine-resistant K1 strain of *P. falciparum* in a murine model. These compounds chelated with the free iron of heme *via* hydrazone functionality to display antimalarial activities. The SAR analysis confirmed the supremacy of the benzothiazole nucleus for the antimalarial activity of these compounds. Interestingly, the *in vitro* and *in vivo* toxicity assays confirmed nominal modification in the biochemical and hematological parameters compared to the control.<sup>149</sup> Shah *et al.* designed a novel library of compounds containing benzothiazole scaffold (**121a–h**, Fig. 20) with significant inhibitory potential against falcipain and cysteine proteases of *P. falciparum* with IC<sub>50</sub> in the range of 11.14–35.70 μM. The molecular docking investigations confirmed the interaction of these derivatives with polar residues buried in the S2 pockets of falcipain-2 and -3 enzymes.<sup>150</sup> However, the *in vivo* investigations suggested that majority of the test compounds specifically inhibited FP-2 but not FP-3 owing to their inability to block the development of the parasite, as deletion of only FP-2 by gene knockout was not lethal to the parasites. Adams *et al.* procured a novel series of ferrocenyl-containing benzothiazoles with amine side-chains (**122**, Fig. 20) and evaluated their antiplasmodial activity against both chloroquine-sensitive (NF54) and chloroquine-resistant (Dd2) strains of *P. falciparum*. The compounds exhibited brilliant antiplasmodial activities in the range of 0.1–1.9 μM along with mild cytotoxicity against Chinese hamster ovarian (CHO) cell line. The compounds also inhibited the formation of β-hematin, although the effect was mild. In addition, the studies concluded that the folded conformation of ferroquine due to hydrogen bonding between the terminal nitrogen atom and the NH on either side of the ferrocenyl moiety resulted in a positive amendment in its properties. This eventually caused significant enhancement in the interactions of these compounds with hematin, further leading to the inhibition of haemozoin formation.<sup>151</sup>

Thakkar *et al.* designed benzothiazole analogues (**123a–c**, **124**; Fig. 20) for *in vitro* evaluation of antimalarial activity through DHFR (dihydrofolate reductase) enzyme inhibition, and to appraise the *in vitro* cytotoxicity and genotoxicity of the molecules against *S. pombe* cells. SAR analysis suggested that the test compounds substituted at the phenyl ring displayed most potent activities against *P. falciparum*. The *in silico* molecular docking investigations showed significant interactions with the active site of binding sites of Pf-DHFR, principally through H-bonding. The IC<sub>50</sub> of the test compounds for DHFR inhibition was in the range of 0.0312–0.0531 μM.<sup>152</sup> Alborz *et al.* performed a highly diastereoselective synthesis of novel benzothiazole-substituted β-lactam hybrids (**125a–f**, Fig. 20) and evaluated their antiparasitic potential against the chloroquine-resistant

K1 strain of *P. falciparum*. The compounds showed significant parasitic inhibition with IC<sub>50</sub> in the range of 6–10 μM. The antimalarial data revealed that methoxyphenyl or ethoxyphenyl substitution on the β-lactam ring makes it highly potent against the malarial parasite. Moreover, the hemolytic activity and mammalian cell toxicity survey of the compounds showed their potential as a medicine. Moreover, the compounds exhibited negligible cytotoxicity on hepatocellular carcinoma cell line (HepG2). The compounds also displayed no significant destructive effect on red blood cells (RBC) as the incubation of cells for 60 minutes at 37 °C revealed only <3% of lysed cells.<sup>153</sup>

## 4. Conclusion

Owing to the concurrent failure of traditional antimalarial drugs, contemporary antimalarial chemotherapy incorporates the utilization of novel scaffolds and/or a comprehensive modification of the existing antimalarial moieties. The ‘azole’ skeleton presents exciting bioactivities owing to the functional similarity of its analogues with several functional groups as well as heterocycles. The bioisosteric potential of an azole motif as well as its analogues makes this ring system an effective substitute for maneuvering the profile of desirable functionalities, thereby improving the overall biological as well as physicochemical profile of the resulting compounds. In addition, the presence of a large number of azole analogues in a variety of ring systems also provides profitable opportunities to investigate the structure activity relationships and pharmacokinetics of future synthetic therapeutics among the already saturated antimalarial chemotherapy. Moreover, the integration of the azole motif in several commercialized drugs necessitates a comprehensive acknowledgement of this ubiquitous scaffold.

## Conflicts of interest

There are no conflicts of interest to declare.

## Acknowledgements

PP and MS duly acknowledge the Department of Chemistry, University of Petroleum & Energy Studies, Dehradun; Department of Chemistry, Uttarakhand University, Dehradun, for providing the research facilities. Sincere thanks to the Department of Chemistry, Guru Nanak Dev University, Amritsar, for providing the state-of-the-art research infrastructure.

## References

- 1 D. J. Gubler, *Emerging Infect. Dis.*, 1998, **4**, 442–450.
- 2 J. A. Turner, C. N. Ruscoe and T. R. Perrior, *Chimia*, 2016, **70**, 684–693.
- 3 R. W. Sutherst, *Clin. Microbiol. Rev.*, 2004, **17**, 136–173.
- 4 N. J. White, *J. Clin. Invest.*, 2004, **113**, 1084–1092.
- 5 WHO facts sheet 2017: Vector Borne Diseases, <https://www.who.int/news-room/fact-sheets/detail/vector-borne-diseases>.

- 6 WHO World Malaria Report 2018, <https://www.who.int/malaria/publications/world-malaria-report-2018/en/>.
- 7 B. Blasco, D. Leroy and D. A. Fidock, *Nat. Med.*, 2017, **23**, 917–928.
- 8 J. K. Baird, N. Valencha, S. Duparc, N. J. White and R. N. Price, *Am. J. Trop. Med. Hyg.*, 2016, **95**, 35–51.
- 9 I. Mueller, P. A. Zimmerman and J. C. Reeder, *Trends Parasitol.*, 2007, **23**, 278–283.
- 10 K. Bruxvoort, C. Goodman, S. P. Kachur and D. Schellenberg, *PLoS One*, 2014, **9**, e84555.
- 11 A. L. Baggish and D. R. Hill, *Antimicrob. Agents Chemother.*, 2002, **46**, 1163–1173.
- 12 M. Rottman and C. McNamara, *et al.*, *Science*, 2010, **329**, 1175–1180.
- 13 N. J. White and T. T. Duong, *et al.*, *N. Engl. J. Med.*, 2016, **12**, 1152–1160.
- 14 (a) M. A. Biamonte, J. Wanner and K. G. Le Roch, *Bioorg. Med. Chem. Lett.*, 2013, **23**, 2829–2843; (b) P. M. Cheuka, N. Lawrence, D. Taylor, S. Wittlin and K. Chibale, *Med. Chem. Commun.*, 2018, **9**, 1733–1745; (c) J. Okombo and K. Chibale, *Med. Chem. Commun.*, 2018, **9**, 437–453; (d) G. Kaur, K. Singh, E. Pavadai and M. Njoroge, *et al.*, *Med. Chem. Commun.*, 2015, **6**, 2023–2028; (e) K. Singh, G. Kaur, F. Mjambili, P. J. Smith and K. Chibale, *Med. Chem. Commun.*, 2014, **5**, 165–170; (f) S. Vandekerckhove, S. D. Moor, D. Segers, C. de Kock, P. J. Smith, K. Chibale, N. D. Kimpe and M. D'Hooghe, *Med. Chem. Commun.*, 2013, **4**, 724–730; (g) K. Kowouvi and B. Alies, *et al.*, *RSC Adv.*, 2019, **9**, 18844–18852; (h) R. Raj, K. M. Land and V. Kumar, *RSC Adv.*, 2015, **5**, 82676–82698.
- 15 E. Fernandez-Alvaro, W. D. Hong, G. L. Nixon, P. M. O'Neill and F. Calderon, *J. Med. Chem.*, 2016, **59**, 5587–5603.
- 16 (a) P. Sidorov, I. Desta, M. Chesse, D. Horvath and G. Marcou, *et al.*, *ChemMedChem*, 2016, **11**, 1339–1351; (b) E. O. J. Porta and I. B. Verdager, *et al.*, *Med. Chem. Commun.*, 2019, **10**, 1599–1605.
- 17 (a) F. W. Muregi and A. Ishih, *Drug Dev. Res.*, 2010, **71**, 20–32; (b) B. Aneja, B. Kumar, A. M. Jairajpuri and M. Abid, *RSC Adv.*, 2016, **6**, 18364–18406.
- 18 C. Kebaier, T. Voza and J. Vanderberg, *PLoS Pathog.*, 2009, **5**, e1000399.
- 19 J. E. Garcia, A. Puentes and M. E. Patarroyo, *Clin. Microbiol. Rev.*, 2006, **19**, 686–707.
- 20 F. B. Cogswell, *Clin. Microbiol. Rev.*, 1992, **10**, 26–35.
- 21 D. C. Anderson, S. A. Lapp, S. Akinyi, E. V. S. Meyer, J. W. Barnwell, C. Korir-Morrison and M. R. Galinski, *J. Proteomics*, 2015, **115**, 157–176.
- 22 D. H. Kerlin and M. L. Gatton, *PLoS One*, 2013, **8**, e57434.
- 23 D. A. Baker, *Mol. Biochem. Parasitol.*, 2010, **172**, 57–65.
- 24 R. A. Kaplan, S. H. Zwiers and G. Yan, *Exp. Parasitol.*, 2001, **98**, 115–122.
- 25 A. S. I. Aly, A. M. Vaughan and S. H. I. Kappe, *Annu. Rev. Microbiol.*, 2009, **63**, 195–221.
- 26 M. M. Mota, G. Pradel, J. P. Vanderberg, J. C. R. Hafalla, U. Frevert, R. S. Nussenzweig, V. Nussenzweig and A. Rodriguez, *Science*, 2001, **291**, 141–144.
- 27 M. Delves, D. Plouffe, C. Scheurer, S. Meister, S. Wittlin, E. A. Winzeler, R. E. Sinden and D. Leroy, *PLoS Med.*, 2012, **9**, e1001169.
- 28 N. J. White, T. T. Hien and F. H. Nosten, *Trends Parasitol.*, 2015, **31**, 607–610.
- 29 A. M. Gopalakrishnan and N. Kumar, *Antimicrob. Agents Chemother.*, 2015, **59**, 317–325.
- 30 S. R. Meshnick, *Int. J. Parasitol.*, 2002, **32**, 1655–1660.
- 31 L. Cui, Z. Wang, J. Miao, M. Miao, R. Chandra, H. Jiang, X.-Z. Su and L. Cui, *Mol. Microbiol.*, 2012, **86**, 111–128.
- 32 M. Cairns, B. Cisse, C. Sokhna, C. Cames, K. Simondon, E. H. Ba, J.-F. Trape, O. Gaye, B. M. Greenwood and P. J. M. Milligan, *Antimicrob. Agents Chemother.*, 2010, **54**, 1265–1274.
- 33 T. M. Davis, T. Y. Hung, I. K. Sim, H. A. Karunajeewa and K. F. Llett, *Drugs*, 2005, **65**, 75–87.
- 34 S. L. Croft, S. Duparc, S. J. Arbe-Barnes, J. C. Craft, C.-S. Shin, L. Fleckenstein, I. Borghini-Fuhrer and H.-J. Rim, *Malar. J.*, 2012, **11**, 270.
- 35 A. F. Slater, *Pharmacol. Ther.*, 1993, **57**, 203–235.
- 36 D. Fernando, C. Rodrigo and S. Rajapakse, *Malar. J.*, 2011, **10**, 351.
- 37 N. Mehrotra, J. Lal, S. K. Puri, K. P. Madhusudanan and R. C. Gupta, *Biopharm. Drug Dispos.*, 2007, **28**, 209–227.
- 38 M. G. V. Lacerda, A. Llanos-Cuentas and S. Krudsood, *et al.*, *N. Engl. J. Med.*, 2019, **380**, 215–228.
- 39 E. R. Lozovsky, T. Chookajorn and K. M. Brown, *et al.*, *Proc. Natl. Acad. Sci. U. S. A.*, 2009, **106**, 12025–12030.
- 40 J. F. Ryley, *Br. J. Pharmacol. Chemother.*, 1953, **8**, 424–430.
- 41 K. Basore, Y. Cheng, A. K. Kushwaha, S. T. Nguyen and S. A. Desai, *Front. Pharmacol.*, 2015, **6**, 91.
- 42 S. Vinayak, M. T. Alam, T. M. Hayden, A. M. Mc. Collum, R. Sem, N. K. Shah and P. Lim, *et al.*, *PLoS Pathog.*, 2010, **6**, e1000830.
- 43 F. Ezzet, M. van Vugt, F. Nosten, S. Looareesuwan and N. J. White, *Antimicrob. Agents Chemother.*, 2000, **44**, 697–704.
- 44 D. L. Wesche, B. G. Schuster, W.-X. Wang and R. L. Woosley, *Clin. Pharmacol. Ther.*, 2000, **67**, 521–529.
- 45 K. J. Palmer, S. M. Holliday and R. N. Brogden, *Drugs*, 1993, **45**, 430–475.
- 46 J. Achan, A. O. Talisuna and A. Erhart, *et al.*, *Malar. J.*, 2011, **10**, 144.
- 47 N. K. Shah, G. P. S. Dhillon, A. P. Dash, U. Arora, S. R. Meshnick and N. Valecha, *Lancet Infect. Dis.*, 2011, **11**, 57–64.
- 48 A. M. Thu, A. P. Phyto, J. Landier, D. M. Parker and F. H. Nosten, *FEBS J.*, 2017, **284**, 2569–2578.
- 49 A. B. S. Sidhu, D. Verdier-Pinard and D. A. Fidock, *Science*, 2002, **298**, 201–213.
- 50 M. Chinnapi, A. Via, P. Marcatili and A. Tramontano, *PLoS One*, 2010, **5**, e14064.
- 51 B. A. Akhoun, K. P. Singh, M. Varshney, S. K. Gupta, Y. Shukla and S. K. Gupta, *PLoS One*, 2014, **15**, e110041.
- 52 R. N. Price, A.-C. Uhlemann and A. Brockmann, *et al.*, *Lancet*, 2004, **364**, 438–447.

- 53 T. Triglia and A. F. Cowman, *Drug Resist. Updates*, 1999, **2**, 15–19.
- 54 R. M. Fairhurst and A. M. Dondorp, *Microbiol. Spectrum*, 2016, **4**, EI10-0013.
- 55 M. A. Phillips, J. Lotharius and K. Marsh, *et al.*, *Sci. Transl. Med.*, 2016, **7**, 296ra111.
- 56 E. L. Flannery, A. K. Chatterjee and E. A. Winzeler, *Nat. Rev. Microbiol.*, 2013, **11**, 849–862.
- 57 T. Triglia and A. F. Cowman, *Drug Resist. Updates*, 1999, **2**, 15–19.
- 58 V. Baraka and D. S. Ishengoma, *et al.*, *Malar. J.*, 2015, **14**, 439.
- 59 W. H. Wernsdorfer and H. Noedl, *Curr. Opin. Infect. Dis.*, 2003, **16**, 553–558.
- 60 C. Karema and M. Imwong, *et al.*, *Antimicrob. Agents Chemother.*, 2010, **54**, 477–483.
- 61 P. Berzosa, A. E-Cantos and L. Garcia, *et al.*, *Malar. J.*, 2017, **16**, 28.
- 62 J. Vanichtanankul, S. Taweechai, C. Uttamapinant, P. Chitnumsub, T. Vilaivan, Y. Yuthavong and S. Kamchonwongpaisana, *Antimicrob. Agents Chemother.*, 2012, **56**, 3928.
- 63 Z. O. Ibraheem, R. A. Majid, S. M. Noor, H. M. Sedik and R. Basir, *Malar. Res. Treat.*, 2014, **2014**, 950424.
- 64 R.-M. Zhou, H.-W. Zhang and C.-Y. Yang, *Malar. J.*, 2016, **15**, 265.
- 65 E. Achol, S. Ochaya, G. M. Malinga, H. Edema and R. Echodu, *BMC Res. Notes*, 2019, **12**, 235.
- 66 N. T. Huy, Y. Shima, A. Maeda, T. T. Men, K. Hirayama, A. Hirase, A. Miyazawa and K. Kamei, *PLoS One*, 2013, **8**, e70025.
- 67 R. Tripathi, A. Rizvi, S. K. Pandey, H. Dwivedi and J. K. Saxena, *Acta Trop.*, 2013, **126**, 150–155.
- 68 M. A. Pfaller and D. J. Krogstad, *J. Infect. Dis.*, 1981, **144**, 372–375.
- 69 T. Tiffert, H. Ginsburg, M. Krugliak, B. C. Elford and V. L. Lew, *Proc. Natl. Acad. Sci. U. S. A.*, 2000, **97**, 331–336.
- 70 N. T. Huy, K. Kamei, Y. Kondo, S. Serada, K. Kanaori, R. Takano, K. Tajima and S. Hara, *J. Biochem.*, 2002, **131**, 437–444.
- 71 V. L. Lew, T. Tiffert and H. Ginsburg, *Cell*, 2002, **18**, P156.
- 72 N. T. Huy, K. Kamei, T. Yamamoto, Y. Kondo, K. Kanaori, R. Takano, K. Tajima and S. Hara, *J. Biol. Chem.*, 2002, **277**, 4152–4158.
- 73 P. D. Crowley and H. C. Gallagher, *J. Appl. Microbiol.*, 2014, **117**, 611–617.
- 74 R. Chandra and S. K. Puri, *Parasitol. Res.*, 2015, **114**, 1239–1243.
- 75 E. H. Jung, D. J. Meyers, J. Bosch and A. Casadevall, *mSphere*, 2018, **3**, e00537.
- 76 N. T. Huy, R. Takano, S. Hara and K. Kamei, *Biol. Pharm. Bull.*, 2004, **27**, 361–365.
- 77 T. E. Wellems, E. P. Rock, W. L. Maloy, D. W. Taylor and R. J. Howard, *UCLA Symp. Mol. Cell. Biol.*, 1987, **42**, 47.
- 78 F. Ardeshir, J. E. Flint, Y. Matsumoto, M. Aikawa, R. T. Reese and H. Stanley, *EMBO J.*, 1987, **6**, 1421.
- 79 A. Kilejian, *Proc. Natl. Acad. Sci. U. S. A.*, 1979, **76**, 4650.
- 80 S. K. Martin, G. H. Rajasekariah, G. Awinda, J. Waitumbi and C. Kifude, *Am. J. Trop. Med. Hyg.*, 2009, **80**, 516–522.
- 81 D. F. Torrence, R. M. Friedmann, K. L. Kirk, L. A. Cohen and C. R. Creveling, *Biochem. Pharmacol.*, 1979, **28**, 1565.
- 82 R. Jain, B. Avramovitch and L. A. Cohen, *Tetrahedron*, 1998, 3235–3242.
- 83 R. Jain, S. Vangapandu, M. Jain, N. Kaur, S. Singh and P. P. Singh, *Bioorg. Med. Chem. Lett.*, 2002, **12**, 1701–1704.
- 84 L. Adane and P. V. Bharatam, *J. Mol. Model.*, 2011, **17**, 657–667.
- 85 A. J. Lin, Q. Zhang, J. Guan and W. K. Milhous, 2-Guanidinylimidazolidinedione Compounds of Making and Using Thereof, *US Pat.*, 7101902, September 5, 2006.
- 86 Q. Zhang, J. Guan, J. Sacci, A. Ager, W. Ellis, W. Milhous, D. Kyle and A. J. Lin, *J. Med. Chem.*, 2005, **48**, 6472–6481.
- 87 J. Guan, X. Wang, K. Smith and A. Ager, *et al.*, *J. Med. Chem.*, 2007, **50**, 6226–6231.
- 88 L. M. Sturk, J. L. Brock, C. R. Bagnell, J. E. Hall and R. R. Tidwell, *Acta Trop.*, 2004, **91**, 131.
- 89 L. Zhang, R. Sathunuru, T. L. Luong, V. Melendez, M. P. Kozar and A. J. Lin, *Bioorg. Med. Chem.*, 2011, **19**, 1541–1549.
- 90 X. Liu and X. Wang, *et al.*, *J. Med. Chem.*, 2011, **54**, 4523–4535.
- 91 L. Zhang and R. Sathunuru, *et al.*, *J. Med. Chem.*, 2011, **54**, 6634–6646.
- 92 K. Sharma, A. Srivastava, R. N. Mehra, G. S. Deora, M. M. Alam, M. S. Zaman and M. Akhter, *Arch. Pharm.*, 2018, **351**, 1700251.
- 93 H. D. Attram, S. Wittlin and K. Chibale, *MedChemComm*, 2019, **10**, 450–455.
- 94 J. A. Romero, M. E. Acosta, N. D. Gamboa, M. R. Mijares, J. B. Sanctis and L. J. Llovera, *Med. Chem. Res.*, 2019, **28**, 13–27.
- 95 P. Toro, A. H. Klahn and B. Pradines, *et al.*, *Inorg. Chem. Commun.*, 2013, **35**, 126–129.
- 96 J. Camacho and A. Barazarte, *et al.*, *Bioorg. Med. Chem.*, 2011, **19**, 2023–2029.
- 97 K. D. Patel, R. H. Vekariya, N. P. Prajapati, D. B. Patel, H. D. Patel, T. Shaikh, D. P. Rajani, S. Rajani, N. S. Shah and D. Jhala, *Arabian J. Chem.*, 2018, DOI: 10.1016/j.arabjc.2018.02.017.
- 98 A. J. Ndakala, R. K. Gessner, P. W. Gitari, N. October, K. L. White, A. Hudson, F. Fakorede, D. M. Shakleford, M. Kaiser, C. Yeates, S. A. Charman and K. Chibale, *J. Med. Chem.*, 2011, **54**, 4581–4589.
- 99 J. Okombo, C. Brunshwig, K. Singh, G. A. Dziwornu, L. Bernard, M. Njoroge, S. Wittlin and K. Chibale, *ACS Infect. Dis.*, 2019, **5**, 372–384.
- 100 K. Singh, J. Okombo, C. Brunshwig, F. Ndubi, L. Bernard and C. Wilkinson, *et al.*, *J. Med. Chem.*, 2017, **60**, 1432–1448.
- 101 J. N. Dominguez, J. E. Charris, M. Caparelli and F. Riggione, *Arzneimittelforschung*, 2002, **52**, 482–488.
- 102 S. Kumar, G. Kumar, M. Kapoor, A. Surolia and N. Surolia, *Synth. Commun.*, 2006, **36**, 215–226.

- 103 A. A. Bekhit, A. Hymete, H. Asfaw and A. E. A. Bekhit, *Arch. Pharm. Chem. Life Sci.*, 2012, **345**, 147–154.
- 104 A. B. Vaidya, J. M. Morrissey and Z. Zhang, *et al.*, *Nat. Commun.*, 2014, **5**, 5521.
- 105 K. Kirk, *Physiol. Rev.*, 2001, **81**, 495–537.
- 106 S. A. Desai, *Cell. Microbiol.*, 2012, **14**, 1003–1009.
- 107 P. Kumar, K. Kadyan, M. Duhan, J. Sindhu, V. Singh and B. S. Saharan, *Chem. Cent. J.*, 2017, **11**, 115.
- 108 P. Prasad, A. G. Kalola and M. P. Patel, *New J. Chem.*, 2018, **42**, 12666–12676.
- 109 A. A. Bekhit, M. N. Saudi and A. M. M. Hassan, *et al.*, *Eur. J. Med. Chem.*, 2018, **163**, 353–366.
- 110 P. N. Kalaria, S. P. Satasia and D. K. Raval, *New J. Chem.*, 2014, **38**, 2902–2910.
- 111 P. N. Kalaria, S. P. Satasia and D. K. Raval, *Eur. J. Med. Chem.*, 2014, **78**, 207–216.
- 112 P. N. Kalaria, S. P. Satasia and D. K. Raval, *New J. Chem.*, 2014, **38**, 1512–1521.
- 113 A. A. Bekhit, A. M. Hassan, H. A. Abd El Razik and M. M. El-Miligy, *et al.*, *Eur. J. Med. Chem.*, 2015, **94**, 30–44.
- 114 A. Marella, M. Shaquiquzaman, M. Akhter, G. Verma and M. M. Alam, *J. Enzyme Inhib. Med. Chem.*, 2015, **30**, 597–606.
- 115 G. Kumar, O. Tanwar, J. Kumar, M. Akhter, S. Sharma, C. R. Pillai, M. M. Alam and M. S. Zama, *Eur. J. Med. Chem.*, 2018, **149**, 139–147.
- 116 A. Jain and P. Piplani, *Mini-Rev. Med. Chem.*, 2019, **19**, 1298–1368.
- 117 P. Prasher and M. Sharma, *Med. Chem. Commun.*, 2019, **10**, 1302–1328.
- 118 M. D'hooghe, S. Vandekerckhove, K. Mollet and K. Vervisch, *et al.*, *Beilstein J. Org. Chem.*, 2011, **7**, 1745–1752.
- 119 S. Balabadra, M. Kotni, V. Manga, A. D. Allanki, R. Prasad and P. S. Sijwali, *Bioorg. Med. Chem.*, 2017, **25**, 221–232.
- 120 V. Patil, W. Guerrant, P. C. Chen, B. Gryder, D. B. Benicewicz, S. I. Khan, B. L. Tekwani and A. K. Oyelere, *Bioorg. Med. Chem.*, 2010, **18**, 415–425.
- 121 X.-M. Chu, C. Wang, W.-L. Wang, L.-L. Liang, W. Liu, K.-K. Gong and K.-L. Sun, *Eur. J. Med. Chem.*, 2019, **166**, 206–223.
- 122 N. Devender, S. Gunjan, S. Chhabra and K. Singh, *et al.*, *Eur. J. Med. Chem.*, 2016, **109**, 187–198.
- 123 A. Kaushansky, A. S. Ye, L. S. Austin, S. A. Mikolajczak, A. M. Vaughan, N. Camargo, P. G. Metzger, A. N. Douglass, G. MacBeath and S. H. I. Kappe, *Cell Rep.*, 2013, **3**, 630–637.
- 124 K. Kumar, B. Pradines, M. Madamet, R. Amalvict and V. Kumar, *Eur. J. Med. Chem.*, 2014, **86**, 113–121.
- 125 N. Boechat, M. L. Ferreira and L. C. S. Pinheiro, *et al.*, *Chem. Biol. Drug Des.*, 2014, **84**, 325–332.
- 126 M. C. Joshi, K. J. Wicht, D. Taylor, R. Hunter, P. J. Smith and T. J. Egan, *Eur. J. Med. Chem.*, 2013, **69**, 338–347.
- 127 L. Taleli, C. Kock, P. J. Smith and S. C. Pelly, *et al.*, *Bioorg. Med. Chem.*, 2015, **23**, 4163–4171.
- 128 S. Manohar, S. I. Khan and D. S. Rawat, *Chem. Biol. Drug Des.*, 2011, **78**, 124–136.
- 129 E. M. Guantai, K. Ncokazi, T. J. Egan, J. Gut, P. J. Rosenthal, P. J. Smith and K. Chibale, *Bioorg. Med. Chem.*, 2010, **18**, 8243–8256.
- 130 R. Kant, D. Kumar, D. Agarwal, R. D. Gupta, R. Tilak, S. K. Awasthi and A. Agarwal, *Eur. J. Med. Chem.*, 2016, **113**, 34–49.
- 131 M. Thillainayagam, K. Malathi and S. Ramaiah, *J. Biomol. Struct. Dyn.*, 2018, **36**, 3993–4009.
- 132 C. Gao, L. Chang, Z. Hu, X.-F. Yan, C. Ding, F. Zhao, X. Wu and L.-S. Feng, *Eur. J. Med. Chem.*, 2019, **163**, 404–412.
- 133 C. Biot, H. Bauer, R. H. Schirmer and E. D. Charvet, *J. Med. Chem.*, 2004, **47**, 5972–5983.
- 134 M. Tukulula, M. Njoroge, G. C. Mugumbate, J. Gut, P. J. Rosenthal, S. Barteau, J. Streckfuss, O. Heudi, J. K. Tchudji and K. Chibale, *Bioorg. Med. Chem.*, 2013, **21**, 4904–4913.
- 135 S. Pandey, P. Agarwal, K. Srivastava, S. R. Kumar, S. K. Puri, P. Verma, J. K. Saxena, A. Sharma, J. Lal and P. M. S. Chauhan, *Eur. J. Med. Chem.*, 2013, **66**, 69–81.
- 136 L. Lobo, L. I. L. Cabral, M. I. Sena and B. Guerreiro, *et al.*, *Malar. J.*, 2018, **17**, 145.
- 137 M. T. Chhabria, S. Patel, P. Modi and P. K. Brahmshatriya, *Curr. Top. Med. Chem.*, 2016, **16**, 2841–2862.
- 138 H. N. Karade, B. N. Acharya, M. Sathe and M. P. Kaushik, *Med. Chem. Res.*, 2008, **17**, 19–29.
- 139 J. M. Bueno, M. Carda, B. Crespo, A. C. Cunat, C. Cozar, M. L. Leon, A. Marco, N. Roda and J. F. Sanz-Cervera, *Bioorg. Med. Chem. Lett.*, 2016, **26**, 3938–3944.
- 140 P. Makam, P. K. Thakur and T. Kannan, *Eur. J. Pharm. Sci.*, 2014, **52**, 138–145.
- 141 D. A. Baker, L. B. Stewart and S. A. Osborne, *Nat. Commun.*, 2017, **8**, 430.
- 142 M. Penzo, L. L. Heras-Duena and L. Mata-Cantero, *et al.*, *Sci. Rep.*, 2019, **9**, 7005.
- 143 D. G. Cabrera, F. Douelle and T.-S. Feng, *et al.*, *J. Med. Chem.*, 2011, **54**, 7713–7719.
- 144 G. A. Patani and E. J. LaVoie, *Chem. Rev.*, 1996, **96**, 3147–3176.
- 145 A. Burger and S. N. Sawhney, *J. Med. Chem.*, 1968, **11**, 270–273.
- 146 E. R. Atkinson and F. E. Granchelli, *J. Pharm. Sci.*, 1975, **65**, 618–620.
- 147 K. Takasu, H. Inoue, H.-S. Kim, M. Suzuki, T. Shishido, Y. Wataya and M. Ihara, *J. Med. Chem.*, 2002, **45**, 995–998.
- 148 S. Hout, N. Azas and A. Darque, *et al.*, *Parasitology*, 2004, **129**, 525–535.
- 149 S. Sarkar, A. A. Siddiqui, S. J. Saha, R. De, S. Mazumder, C. Banerjee, M. S. Iqbal, S. Nag, S. Adhikari and U. Bandopadhyay, *Antimicrob. Agents Chemother.*, 2016, **60**, 4217–4228.
- 150 F. Shah, Y. Wu, J. Gut, Y. Pedduri, J. Legac, P. J. Rosenthal and M. A. Avery, *Med. Chem. Commun.*, 2011, **2**, 1201–1207.
- 151 M. Adams, C. de Kock, P. J. Smith, K. Chibale and G. S. Smith, *Eur. J. Inorg. Chem.*, 2017, **2017**, 242–246.
- 152 S. S. Thakkar, P. Thakor, A. Ray, H. Doshi and V. R. Thakkar, *Bioorg. Med. Chem.*, 2017, **25**, 5396–5406.
- 153 M. Alborz, A. Jarrahpour and R. Pournajati, *et al.*, *Eur. J. Med. Chem.*, 2018, **143**, 283–291.